universität
wien

MASTERARBEIT

Titel der Masterarbeit

“Relative Age of Polygonal Impact Craters on Venus“

Verfasser

Dipl.-Ing Gerhard Weihs BSc

angestrebter akademischer Titel

Master of Science (MSc)

Wien, 2014

Studienkennzahl lt. Studienbuch:	A 066 861
Studienrichtung lt. Studienblatt:	Masterstudium Astronomie
Betreuerin:	Univ.-Prof. Dr. Maria G. Firneis

Acknowledgement

I gratefully acknowledge the thoughtful reviews by Univ.-Prof. Dr. Maria G. Firneis and Mag. Johannes J. Leitner, who significantly helped to improve the content and the style of this manuscript.

Contents

1 Introduction

1.1 Aims of the Study

Craters are the most typical landforms in the inner planetary system. The geological history of the planet can be reconstructed by the number, distribution, and state of preservation of impact craters. The physical properties of the target material and the mechanics of the cratering process can be revealed from the morphology of craters (Wood and Andersson, 1978).

Polygonal impact craters (PICs) are especially shaped craters, where the crater rims are not circular but consists of at least two straight segments. Polygonal impact craters on Venus are well studied by (Öhman et al., 2005; Öhman, 2009; Aittola et al., 2007, 2010), attempting to obtain a better understanding of the process of formation of PICs and its consequences. PICs were studied as a poorly understood natural phenomenon, and partly as a tool to understand the geological evolution.

The goal of this study is to estimate the relative age of polygonal impact craters on Venus, that means in relation to the surrounding geologic structures. Though the absolute age of the Venusian surface is only roughly known (about 500 to 750 Myr), the relative age implies the position of a geological unit in the Venusian stratigraphy.

1.2 Key Facts of Venus

- Distance from Sun: $1.1 \cdot 10^8$ km = 0.72 AU
- Orbit Period: 225 d
- Orbital eccentricity 0.0068
- Orbital inclination 3.394°
- Tilt of axis 177.36°
- Visual geometric albedo 0.65
- Mass ($4.869 \cdot 10^{24}$ kg (0.81 Earth masses)
- Radius: 6052 km (0.95 of Earth radius)
- Rotational Period (sidereal): 243 d (retrograde)
- Average Density: 5.24 kg/m^3 (0.95 times that of Earth)
- Surface Gravity: 8.87 m/s^2 (0.91 times that of Earth)
- Surface Mean Temperature: 737 K (464° C)
- Surface Atmospheric Pressure: (90 ± 2 bar) (92 times that of Earth)
- Atmospheric Composition: Carbon dioxide (96 %); nitrogen (more than 3 %); trace amounts of: sulfur dioxide, water vapor, carbon monoxide, argon, helium, neon, hydrogen chloride, hydrogen fluoride

according to (NASA-Planetary-Fact-Sheet, 2013)

2 Venusian Surface

2.1 Geological Structures on Venusian Surface

First observation of the surface using the radar-echo method from Earth (using the radio telescopes in Arecibo and Goldstone) showed several details. Some regions were highly reflective for radar beams. They could be identified as highlands or mountains and named Alpha Regio, Beta Regio and Maxwell Mons.

The surface area of Venus amounts to $\sim 460 \cdot 10^6\, km^2$ that is about 90 % of that of the Earth, and most of the surface is comparatively smooth (see Figure 2.1), lying within 500 m to either side of the mean planetary radius (MPR = 6,051 km). Venus appears to be almost perfectly spherical.

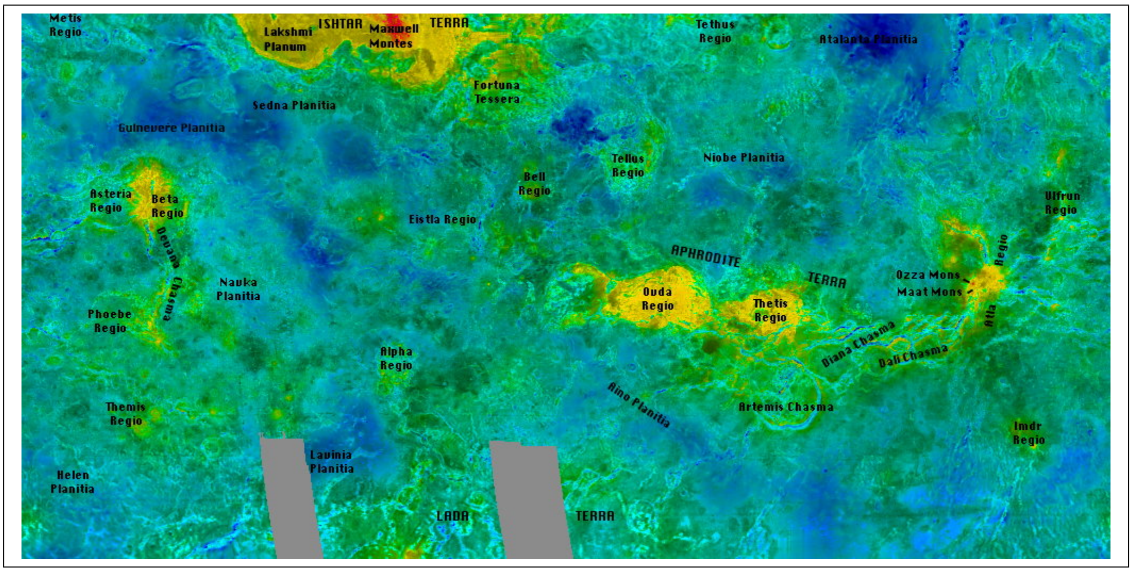

Figure 2.1: Venus topology of the Venusian surface in Mercator projection (credit: Calvin J. Hamilton, http://www.solarviews.com).

2.1.1 Main Elements of the Venusian Surface

The surface consists of four main parts (see examples in Figure 2.2):

- **Volcanic plains** forming the vast majority of the planet, covering about 80 % of the surface.
- **Intensely deformed terrains** like tesserae, ridge belts, mountain belts, and rifts, forming upland plateaus.
- **Coronae**
- **Impact craters**

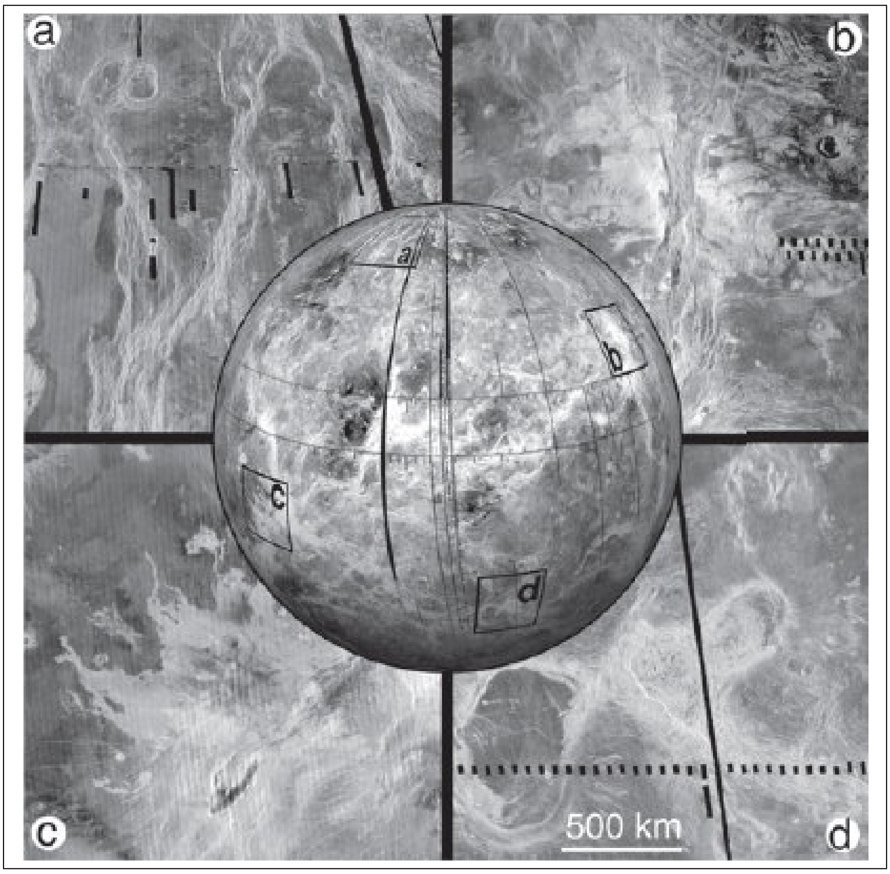

Figure 2.2: Typical terrain types of Venus from Magellan images (a) - (c) and their positions shown on a global mosaic centered at 240°E: (a) belts of low ridges (brighter linear features) and neighboring regional plains (darker background); (b) tessera terrain (radar-bright) of Beta Regio cut by a rift zone; (c) Maat Mons volcano and its radar-bright lava flows; (d) coronae of the Parga Chasmata rift zone (Basilevsky et al., 2003).

2.1.1.1 Volcanic Plains

- Nearly 80 % of the surface are plains, lying close to the mean planetary radius (MPR = 6051.5 km above the planet's center of mass) are **regional plains**, consisting of **plains with wrinkle ridges** and **shield plains**. Plains with wrinkle ridges characterized by ridges, a few km broad, but 100 to 200 km extended. These features indicate the eruptions of liquid, basaltic lava forming the plains, which later were wrinkled by horizontal compressions (Basilevsky et al., 2003). Shield plains are the second kind of regional plains, less dominating, which are forming large fields of volcanic shields, each 5 to 15 km in diameter.
- About 10-15 % of the Venusian plains consist of **lobate plains**, which are younger than the regional plains.
- Another feature within the plains are sinuous **channels**, about 2-5 km wide and extended over hundreds of km (Baker et al., 1997). Most current theses state, that the channels are 'lava channels', a result of thermal erosion by flowing lava.
- On the surface more than 300 **volcanoes** with a diameter between 20 and 100 km in and more than 100 volcanoes >100 km in diameter are known. Maat Mons with 9 km is the highest one.

Table 2.1: Venus Surface Structures - in this table all structures are reported known up to now, as listed in (IAU/USGS/NASA-Planetary-Database, 2013).

Feature-Type	Number	Short Description
Chasma, chasmata	63	deep, long and steep-sided depressions, similar to Earth's trenches
Collis, colles	16	small hills
Corona, coronae	347	ovoid-shaped structures, often similar to craters
Crater, craters	898	circular depressions caused by impacted meteorites
Dorsum, dorsa	103	similar to Earth's ridges
Farrum, farra	10	pancake-like structures
Fluctus, fluctus	51	flow terrains
Fossa, fossae	34	long, narrow and shallow depressions
Labyrinthus, labyrinthi	1	several intersecting valleys
Linea, lineae	24	dark or bright and long markings, either straight or curved
Mons, montes	122	mountains
Patera, paterae	89	irregular or complex craters with scalloped edges
Planitia, planitiae	41	plateaus or high plains
Planum, plana	4	low plains
Regio, regiones	22	huge areas denoted by an different reflectivity than the adjacent area
Rupes, rupes	7	escarpments
Terra, terrae	3	extensive land masses
Tessera, tesserae	64	polygonal terrains, often like tiles
Tholus, tholi	58	small but dominating hills or mountains
Unda, undae	3	dunes
Vallis, valles	72	valleys

2.1.1.2 Intensely Deformed Terrains

Rough terrains, due to tectonic deformations, cover more than 20 % of the surface: ridge belts, fractured plains, tesserae, mountain belts , and rift zones (Basilevsky and Head, 2002b).

- According to Basilevsky et al., 2003 **ridge belts** form a global-wide system, which is not flooded by lava of the surrounding regional plains. These belts are composed of plains-forming material, probably solidified basaltic lava.
- **Densely fractured plains**, building small islands (100-200 km), are overtopping the regional plains by a few hundred meters.
- **Tesserae**, probably the oldest regions on Venus, cover about 8.5 % of the entire surface. Islands and continents are overtopping the surrounding regional plains which embed the tesserae. The surface of a tessera is radar-bright and shows a rough, chaotic pattern of linear ridges and valleys, and probably produced by tectonic forces of compressing and dragging. Tesserae occur especially in Terras and Regios (Ivanov and Head, 1996; Hansen and Willis, 1997; Basilevsky and Head, 2003).
- **Mountain belts** form a specific terrain type (surrounding the Lakshmi Plateau) which consist of clusters of parallel ridges. Maxwell Montes, the highest mountain range on Venus, rises to almost 11 km above the mean planetary radius (Basilevsky and Head, 2003).
- Venusian rifts, also called **Chasmata** are forming a global system about 40,000 km of length with typically troughs with a depth of several km, while the rims are often lifted above the neighboring terrain (Basilevsky and Head, 2003; Schaber, 1982).

2.1.1.3 Coronae

Several hundreds of volcanic features which are unique to Venus, sÃij-called coronae, are observed on the surface of Venus, Coronae, first discovered in the images of the landers Venera 15/16 by Barsukov et al., 1986, are oval or circular features with diameters from 100 to 300 km in or even larger and a circular annulus. According to Stofan et al., 1997 coronae are formed as a result of rising mantle plumes. If the magmatic melt reaches the surface it forms aprons of lava flow. After the cooling down of the plume, the uplifted surface collapses and produces a corona (Stofan et al., 1997; Basilevsky and Head, 2003).

2.1.1.4 Impact Craters

Size-Frequency Distribution of Craters

Venus has almost 900 impact craters of 1.5 - 270 km in diameter (see (IAU/USGS/NASA-Planetary-Database, 2013), and (Schaber et al., 1992; Phillips et al., 1992; Herrick and Phillips, 1994b; Strom et al., 1994; Herrick et al., 1997).

The size-frequency distribution of the impact craters shown in Figure 2.3, is obviously controlled by the massive Venusian atmosphere. The dense atmosphere prevents the smallest projectiles from cratering the surface, usually by breaking them into smaller fragments or by eroding them (Phillips et al., 1991; Herrick and Phillips, 1994a; McKinnon et al., 1997; Cochrane and Ghail, 2006).

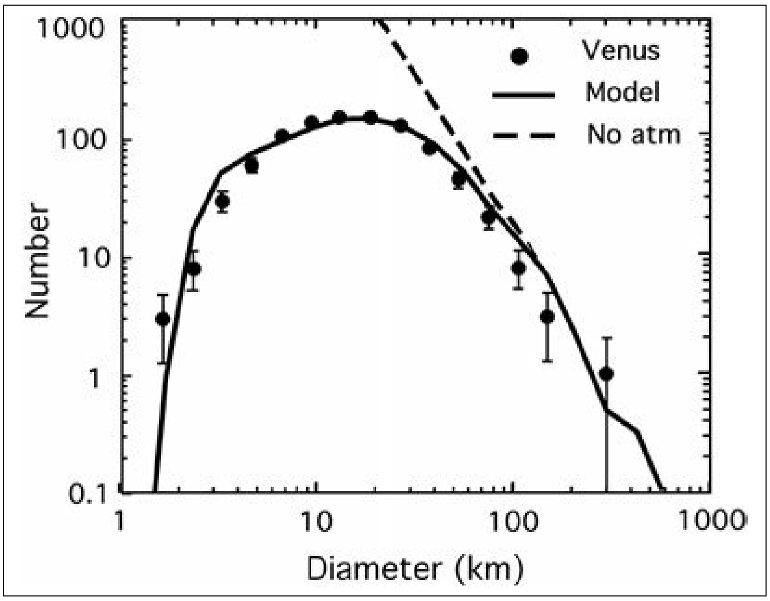

Figure 2.3: The size-frequency distribution (log Number vs. log Diameter) of impact craters on Venus is compared to a model simulating the formation of an 800 Myr old crater population. Plotted is the case of the presence/ absence of today's atmosphere (modified from (McKinnon et al., 1997; Basilevsky and Head, 2003).

3 Geological History of the Venusian Surface

3.1 Short Overview of the Geological History

The interpretation of the geological history of the Venusian surface depends on various authors. In the paper of Basilevsky et al., 2003 six different periods are named. The study follows the more recent paper by Ivanov and Head, 2011 with only four historical eras:

- **Pre-Fortunian** is the earliest phase of the history of the Venusian surface and it predates the observed geological surface features. Its is assumed that remnants may be still existing as deformed rocks. Therefore just 10 % to 20 % of the geological history is observable now (Ivanov and Head, 2011).
- The oldest phase, the so-called **Fortunian Period**, whereby its lower stratigraphic boundary cannot be determined. Intense deformed regions with a thicker crust were built (e.g. tesserae).
- The next period was the **Guineverian Period**, which was characterized by the formation of deformed plains, mountain belts, and the majority of coronae. The later part of the Guineverian Period involves global emplacements of smoothly deformed volcanic plains, followed by the formation of global wrinkle ridges.
- The **Atlian Period** showed the formation of rift zones and lava flows, which were not deformed by wrinkle ridges. Often large shield volcanoes and coronae are associated with it. The assumption that the Atlian volcanism may continue to the present day is still unproved (Ivanov and Head, 2011).

According to Ivanov and Head, 2011 most of the resurfacing of the Venusian surface happened during the Guineverian period, and only the rest of about 16 % in the Atlian Period. This later phase was marked with a reduced rate of volcanism and tectonism and lasted twice the time of the Guineverian period.

In the geological history of the Venusian surface three observations seem to be of great importance:

- There is no evidence that Venus' zones show subduction zones, where the existing crust is recycled into the mantle (Turcotte et al., 1999).
- Corresponding to the grade of cratering, the Venusian surface shows a uniform character (Turcotte et al., 1999).
- The distribution of all impact craters on the entire planet is indistinguishable from a random simulation (Schaber et al., 1992; Turcotte, 1997; Turcotte et al., 1999; Basilevsky and Head, 2003).

3.2 Cratering Statistics

Turcotte et al., 1999 proved that the actual distribution of impact craters on Venus cannot be visually distinguished from random simulations, using the method of pair-correlation statistics [a] suggested by Turcotte, 1997. The authors obtained the statistics for 923 craters on Venus using data from Herrick et al., 1997.

The result showed, that the observed craters distribution is indistinguishable from a random distribution.

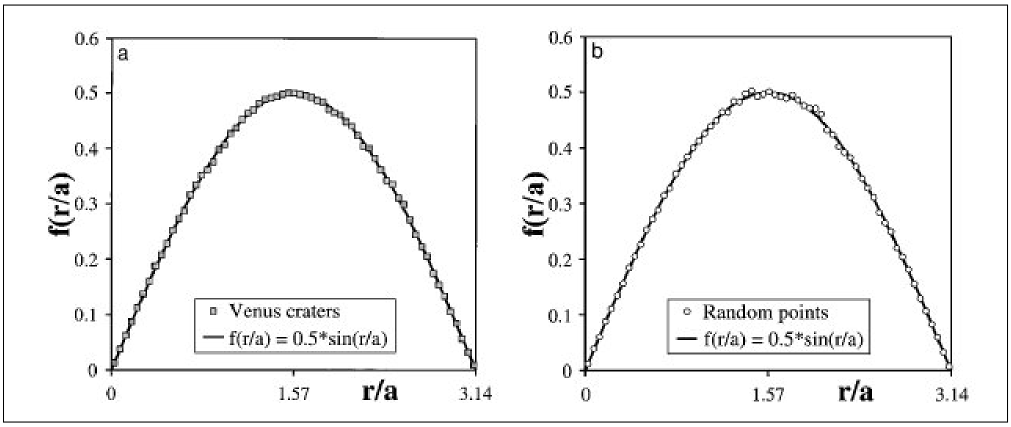

Figure 3.1: (a) Pair-correlation technique applied to 923 craters on Venus, (b) Pair-correlation technique applied to 923 points randomly distributed over a sphere (Turcotte et al., 1999).

To check their method, Turcotte et al., 1999 applied the same analysis to the spatial distribution of coronae on Venus (see Figure 3.2). For the coronae, they found a clear deviations from a random distribution. This indicates flooding by lava, which erased all evidence of earlier craters on large scales (Turcotte et al., 1999).

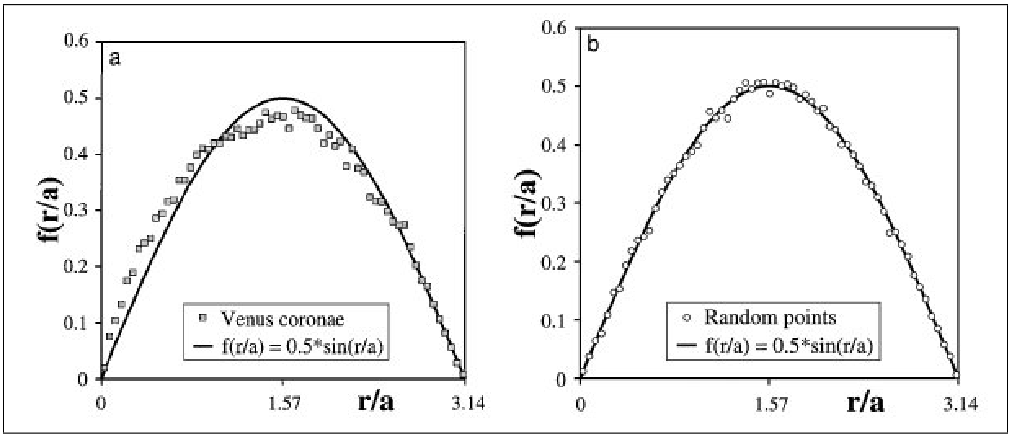

Figure 3.2: (a) Pair-correlation technique applied to 335 coronae on Venus. (b) Pair-correlation technique applied to 335 points randomly distributed over a sphere (Turcotte et al., 1999).

[a] In a pair-correlation statistics the distances from each point to all other points are obtained. For a spherical surface of radius a, the range of distances is from $r = 0$ to $r = \pi a$. If the points are randomly distributed over the sphere, the resulting non-cumulative distribution of distances is proportional to $\sin(r/a)$.

3.3 Global Resurfacing of Venus

3.3.1 Resurfacing Models

Schaber et al., 1992 defined several constraints for resurfacing models out of the detailed investigations of the craters and their distribution on Venus:

- the distribution of the impact craters is indistinguishable from a random one.
- populations of young craters on Mars show a similar size-density distribution of large craters, and the much lower density indicates a mean age of about 0.5 Gyr.
- the density of small craters declines rapidly with decreasing diameters because the dense atmosphere inhibits that small impactors are reaching the surface.
- only 4 % of the impact craters are embayed by lavas.

On Earth or Mars many craters show various states of degradation as a consequence of different deformations (e.g. atmospheric erosion and deposition, fluvial and glacial deposition, or volcanic burial or tectonic deformations), while on Venus a strongly uniform and unique distribution has been found (see Figure 4.1).

Schaber et al., 1992 interpreted the facts in such a way that the planet's cratering record was erased by a global resurfacing events. The latest resurfacing event was terminated about 0.5 Gyr, after which the volcanic activity decreased.

In the crater study Strom et al., 1994 investigated 932 craters on Venus. The crater distribution found is given in Figure 3.3 and yielded clues regarding the resurfacing and the estimated age of the surface.

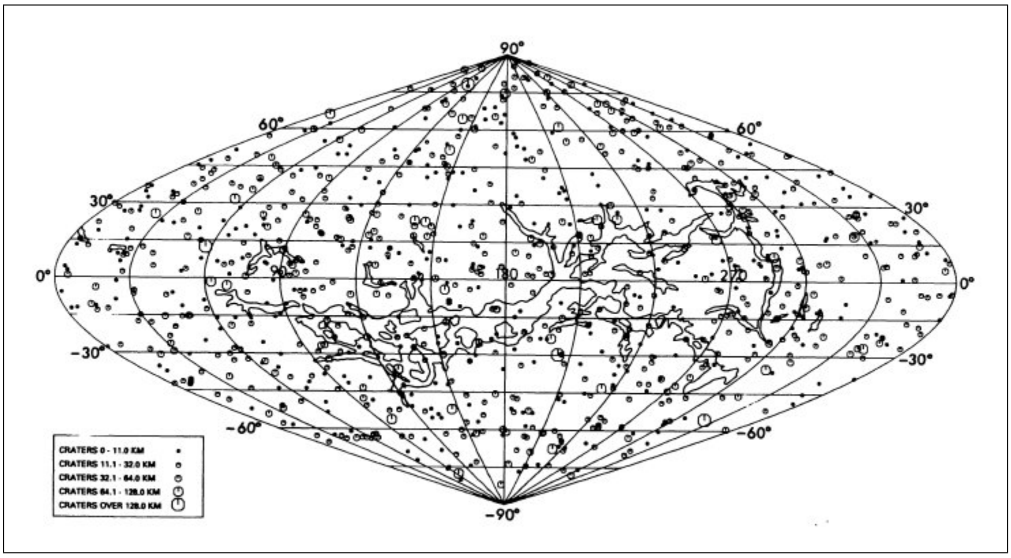

Figure 3.3: Sinusoidal projection of the Venusian surface showing the crater distribution (Strom et al., 1994).

Another rigorous analysis by McKinnon et al., 1997 indicated that the basic model designed by Schaber et al., 1992 is now well accepted by the planetary science community (Strom et al., 1994; Basilevsky et al., 2003).

Whether this surface renewal process was a catastrophic event concerning the whole planet (which perhaps was repeated every 0.5 - 1 Gyr) or whether the volcanic activity decreased over a longer period across a sliding scale, is not yet completely clear.

Generally there exist two resurfacing models for Venus:

- The **regional resurfacing model**, for which the resurfacing is considered as a more or less continuous process.
- The **global resurfacing model**, which means that resurfacing occurred catastrophically and episodically on a global scale.

3.3.2 Standard Model of Venusian Resurfacing

Turcotte et al., 1995, 1997, 1999 proposed a model of global resurfacing with an episodic heat loss from the Venusian interior. This accepted **Standard Model** consists of interchanging active and passive stages.

A graphic presentation of the Standard Model is given in Figure 3.4. The model presents the knowledge of 1993, thus the line "global subduction occurs" at 600 Myr has to be replaced by "local subduction occurs".

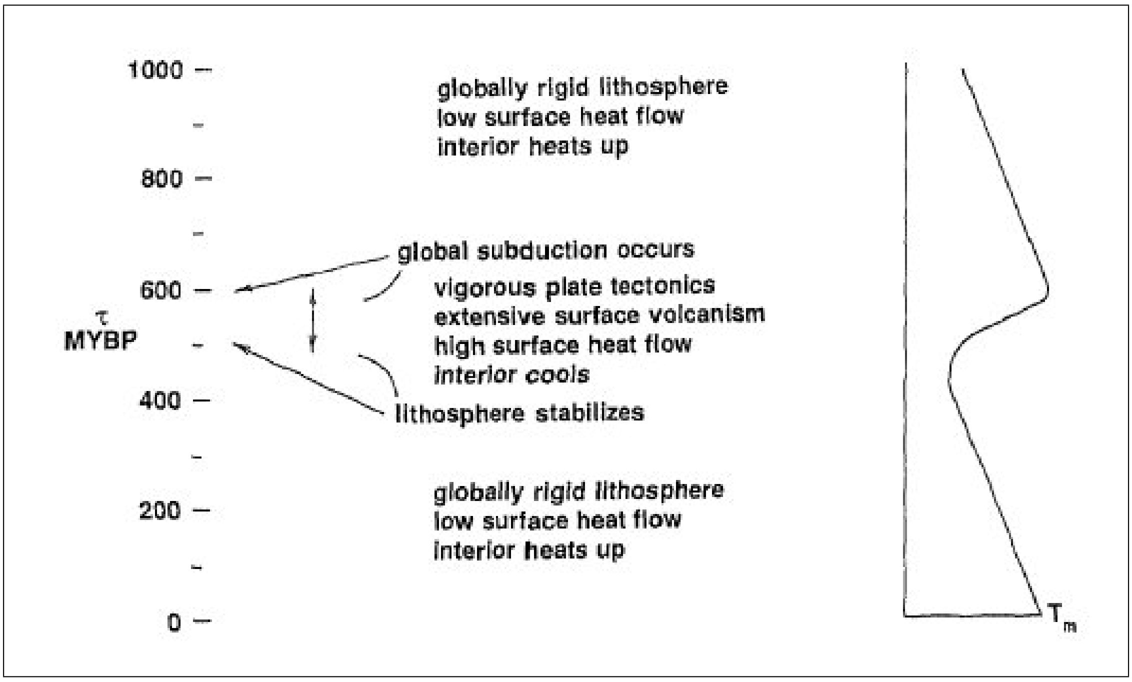

Figure 3.4: Illustration of episodic plate tectonic on Venus for the last Gyr and the qualitative behavior of the mean mantle temperature T_m (Turcotte, 1993).

- The **passive stage** begins with a very low heat flow on the surface. The heat production is due to radioactive elements (elements uranium, thorium, and potassium in concentrations similarly found in Earth), as well as friction heat, gravitational heat, and the heat by phase-transitions. To loose the heat generated, either the heat must be conducted through a the lithosphere or the lithosphere must be treated by a subduction. The alternative is that the temperature within the planet is increasing, then the temperature in the interior and in particular in the lithosphere will increase more and more, and until a threshold temperature is reached, then the lithosphere will become unstable and a new period of global plate subduction is initiated (Turcotte et al., 1999).
- The **active episode** is characterized by an extensive plate-tectonic and a high rate of local subduction. The high surface heat flow lead to a rapid cooling of the planetary interior, and after an active time span of about 100 to 200 Myr the lithosphere became

too cold to support continued plate-recycling. As a consequence the lithospheric plates became stabilized and subsequently only thermal conductivity contributes to a cooling of the interior (Turcotte et al., 1999).

4 Dating Planetary Surfaces

4.1 Methods of Dating Planetary Surfaces

Generally there exist two basic types of dating methods for planetary surfaces:

- an absolute age dating - which determines the time at which a surface or feature is formed.
- a relative age dating - which determines the order, but not the time of formation.

4.1.1 Absolute Dating - Chronology

Depending on the accessibility of the planetary surface two methods of absolute dating are to be distinguished.

- The **method of using radioactive isotopes** is practicable on Earth and on the Moon only. Most rocks contain small amounts of radioactive isotopes, such as ^{238}U, ^{235}U, ^{232}Th and ^{40}K, which decay with known rates, and allows the determination of an absolute age.
- The **method of crater counting** is practicable for extraterrestrial bodies. By counting the total number of craters on a surface or surface unit, and if the rate of crater formation (so-called 'crater production') is known then it is possible to estimate the absolute age of the surface.

4.1.2 Relative Age Dating - Stratigraphy

Though it is not always possible to date a surface on an absolute time scale, we often are able to establish the order in which certain events occurred (the traditional methods of superposition among various geologic units). For example, if lava flows are observed to imbed crater rims, they were emplaced after the formation of these craters.

An alternative method relies on the principle that an older surface has accumulated a greater number of craters than a younger one.

4.2 Chronology - Absolute Age Dating

4.2.1 Using Radioactive Isotopes

Most stones contain amounts of radioactive isotopes with known rates of decay, mainly ^{238}U, ^{235}U, ^{232}Th and ^{40}K. The measured quantity of radioactive isotopes, set in relation to the amount of stable isotopes, enables a calculation of the rock's absolute age. Only terrestrial and lunar rocks and meteorites have been dated using this method.

The content of isotopes in rocks on the Venusian surface was first measured by the landing units of Venera 8, 9 and 10. The values are given in Table 4.1 (Surkov, 1982). The discovery of uranium (U), thorium (Th), and potassium (K) in rocks on the surface of Venus supports the concept, that these rocks were generated by the melting the material inside.

Table 4.1: Content of radioactive isotops in Venusian rocks measured by the Russian landers Venera 8, 9 and 10, compared with the values of rocks on Earth , after (Surkov, 1982).

Rocks	Probe/Rock	Potassium [%]	Uranium [ppm]	Thorium [ppm]
Venus rocks	Venera 8	4.00 ± 1.20	2.20 ± 0.70	6.50 ± 0.20
	Venera 9	0.47 ± 0.08	0.60 ± 0.16	3.65 ± 0.42
	Venera 10	0.30 ± 0.16	0.46 ± 0.26	0.70 ± 0.34
Earth rocks	Basalt	0.76	0.86	2.10
	Granite	3.24	9.04	21.90

The K/U ratio for the Venusian rocks is close to Earth's magmatic rocks (about 10^4), so one can assume, that the processes forming the surface are similar to those operating on Earth (Weitz and Basilevsky, 1993).

4.2.2 Using Crater Counting

Neukum and Ivanov, 1994 provided a concept of determining the absolute age of a planetary surface. The task to obtain an absolute age is to fit:

- the observed crater size-frequency distribution (SFD), restricted to a certain surface unit
- to a known crater production function (PF)
- using a calibrating chronology function (CF).

This concept is roughly explained in Figure 4.1 using the example of Mars.

Production Function PF

> “A production function describes how many impact craters of a certain size are formed related to the number of any other crater size” (Michael and Neukum, 2010).

The production function in Figure 4.1a is a plot, on logarithmic scales, of the cumulative crater-frequency versus crater size ranges, fitted with a polynomial approximation (Michael and Neukum, 2010; Neukum and Ivanov, 1994; Ivanov and Head, 2001) The oldest units are characterized by a larger range of crater sizes and younger units by lesser craters, at least on homogeneous surface units of the Moon or Mars.

The **Neukum presentation** of the production function (Neukum and Ivanov, 1994) is the mostly used form of the PF. The production function is a simple curve on a log(N_{cum})-log(D) plot, and it can easily be approximated with a polynomial function (Ivanov and Head, 2001; Michael and Neukum, 2010) :

$$log(N_{cum}) = p \tag{4.1}$$

$$p = \sum_{i=0}^{n} a_i \; x^i \tag{4.2}$$

$$and \cdots x = log(D) \tag{4.3}$$

for i = 0 ...n , N_{cum} is the cumulative number of craters, D designates the diameter and a_i the coefficients of the polynomial function.

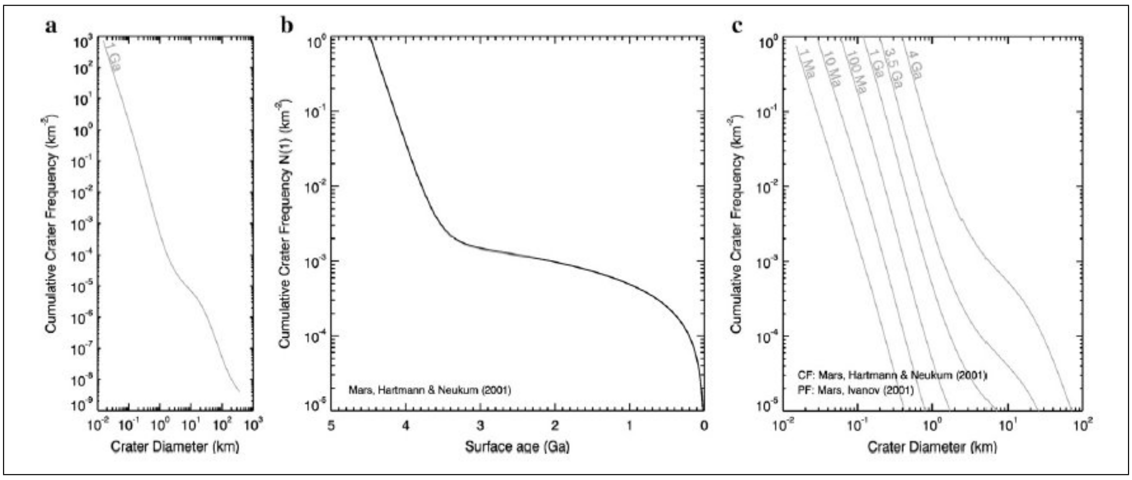

Figure 4.1: Determining the age of Mars' surface by crater counting: (a) Polynomial production function (Neukum and Ivanov, 1994; Ivanov and Head, 2001). (b) Mars chronology function (Hartmann and Neukum, 2001). (c) Mars cumulative crater frequency isochrons (Michael and Neukum, 2010).

The function PF can be expressed in differential form:

$$F = -\frac{dN}{dD} = \frac{dN}{dp}\frac{dp}{dx}\frac{dx}{dD}. \tag{4.4}$$

and after insertion of p and x and integration we get for PF:

$$F = -10^p \; ln10 \cdot \sum_{j=1}^{n} j a_j x^{j-1} \cdot \frac{1}{D \; ln10}, \tag{4.5}$$

$$F = -\frac{1}{D} \cdot 10^{\sum_{i=0}^{n} a_i x^i} \cdot \sum_{j=1}^{n} j a_j x^{j-1}. \tag{4.6}$$

In the Hartmann presentation of the PF, which is non-cumulative, the data are split into bins of width $D(\sqrt{2}-1)$, so the production function takes this form of:

$$H(D) = FD(\sqrt{2}-1) \tag{4.7}$$

$$H(D) = -(\sqrt{2}-1)10^{\sum_{i=0}^{n} a_i x^i} \sum_{j=1}^{n} j a_j x^j. \tag{4.8}$$

Chronology Function CF describes the cratering rate in past times. going back to around 3 Ga, going over into an exponentially increasing rate beyond that time. For Mars the chronology function (Figure 4.1b) can be approximated by a function which describes a constant cratering rate going back to around 3 Gyr (Hartmann and Neukum, 2001).

Isochron Diagram Figure 4.1c shows the cumulative crater size-frequency distribution normalized to a unit area versus the corresponding age. In this way it is possible fit an observed cumulative size-frequency distribution and to read the age from the plot. On the other hand, it is possible to construct the cumulative crater frequency for a given surface age - yielding an isochron diagram (Michael and Neukum, 2010).

Impactor Flux The dating of different planetary surfaces requires a consideration on the cratering rate with respect to the Moon (Ivanov and Head, 2001; Hartmann and Neukum, 2001; Neukum and Ivanov, 2001). This planetary cratering ratios are given in Figure 4.2. The curves for Venus and the Earth for diameters < 10 km are not presented, for the influence of the atmospheric shielding is too important to these range. The present rate of crater formation will be estimated from the observations of various objects crossing the planets's orbit (Michael and Neukum, 2010).

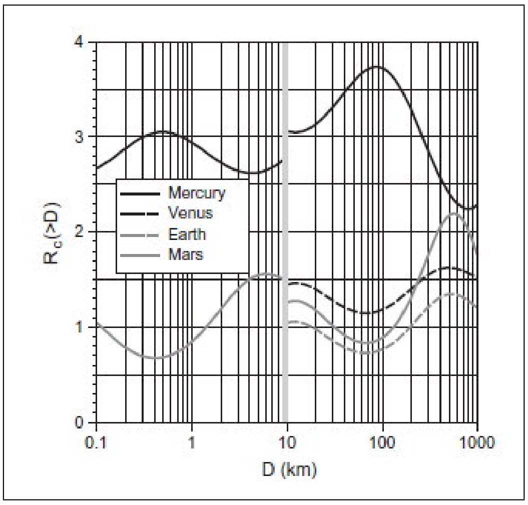

Figure 4.2: Planetary cratering ratios R_c with respect to the Moon, for craters larger than a given diameter D. For Venus and Earth the curves for a diameter less than a diameter of 10 km are not shown because of of the erosion or atmospheric shielding at these sizes (Le Feuvre and Wieczorek, 2011).

5 Impact Cratering Processes

An impact crater will be created if an impactor hits a target with a velocity larger than the velocity of sound of the target (so-called hypervelocity). The produced shock wave generates a crater, which is much larger than the projectile. This shock wave causes an extreme high compression of the target rocks, with pressures which exceed the Hugoniot elastic limit by far. This Hugoniot elastic limit is a material property which describes the maximum stress a material can resist without being permanently deformed (cf. compilations by Roddy, 1977; Melosh, 1989; Melosh and Ivanov, 1999).

The Hugoniot equations for shock fronts connect the uncompressed to the compressed values of pressure P, internal energy E, and density ρ. Values in front of a shock wave are marked with $_0$ (P_0, E_0, ρ_0). The Hugoniot equations can be written as (e.g. Melosh, 1989):

$$\rho(U - u_p) = \rho_0 U \tag{5.1}$$

$$P - P_0 = \rho_0 u_p U \tag{5.2}$$

$$E - E_0 = (P + P_0)(V_0 - V)/2. \tag{5.3}$$

with $V = 1/\rho$ the specific volume, U the velocity of the shock wave und u_p the velocity of the projectile. In addition to these three equations, an equation of state is necessary (cf. (Melosh, 1989)).

The impact of a large meteorite, asteroid, or comet releases a kinetic energy corresponding to $1/2 \cdot mu_p^2$ (m = mass, u_p = velocity of the projectile), where the velocities u_p lie in a range between 11 and 72 km/s. For example the small Meteor Crater in Arizona (1.2 km in diameter) was produced by an iron meteorite with a diameter of about 30-50 m (French, 1998).

According to French, 1998 the energy released during a small impact event, creating craters of 5-10 km in diameter, is about 10^{17}-10^{18} J. A comparable amount of energy was released during the eruption of Mount St. Helens of 1980 with about $6 \cdot 10^{16}$ J and in the great San Francisco earthquake of 1906 with 10^{17} J. The formation of a larger craters (50-200 km in diameter) releases about 10^{21}-10^{23} J.

5.1 The three Stages of Formation of Impact Craters

After Melosh (1989) it is conventional to distinguish three sequential stages of an impact event:

1. **Contact and Compression**
2. **Excavation**
3. **Modification**

(Melosh, 1989; Melosh and Ivanov, 1999).

5.1.1 Contact and Compression

The cratering event starts with the contact of a projectile with hypervelocity with the target material. The kinetic energy is converted into heat and shock waves moving with supersonic

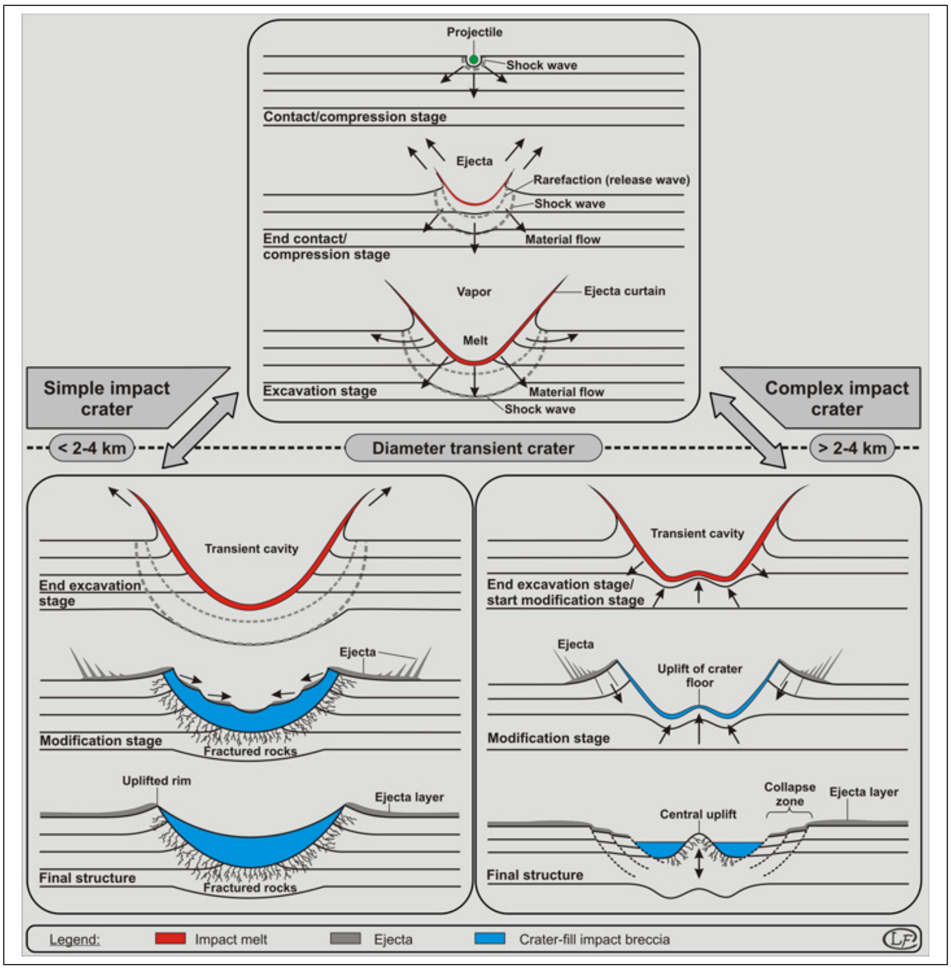

Figure 5.1: The three Stages of Formation of Impact Craters (French, 1998).

speed are transformed into stress waves, and at larger distances, into elastic or seismic waves (Melosh and Ivanov, 1999).

For strong shock waves this compression results in immediate melting or vaporization of the material of the target and the impactor near the impact point (see Figure 5.1). The stage 'contact and compression' is the shortest, lasting only as long as it takes the projectile to enter the target and deposit its energy. (Melosh and Ivanov, 1999).

5.1.2 Excavation

In the excavation stage the generated shock waves expand, compressing the target material and a relaxation wave ejects the material, opening an 'transient crater'. About half of the material is ejected from the crater, the other half slides in some kind of plastic flow into the target (see Figure 5.1). Most of the impact models predict, that the transient crater is shaped like a hemisphere (Melosh and Ivanov, 1999; French, 1998).

5.1.3 Modification

The modification of the transient cavity results in a shallower crater which is more stable. According to Melosh and Ivanov, 1999 the modification mainly depends on the crater size, on the gravity field of the planet and on the strength of near-surface rocks.

5.2 The Final Formation of Craters

5.2.1 Formation of Simple Craters

According to Melosh and Ivanov, 1999 two different mechanisms alter the shape of the transient crater:

> "Dry friction leads to the continued growth of the transient cavity diameter after the moment when the cavity depth reaches its final value, slumping of the steep transient cavity walls under the force of gravity" (Melosh and Ivanov, 1999).

The result is a bowl-shaped crater with a typical ratio of depth/diameter of about 1:5 or 1:4 .

5.2.2 Formation of Complex Craters

The process of the modification of complex craters is referred to as 'transient crater collapse' (Melosh and Ivanov, 1999). Complex craters are shallower than simple craters and the center of the floor is uplifted creating a central peak or mound. The remaining parts of the carter are filled with breccia.

Studies of lunar complex craters have shown that the inner walls of rims acts like a plastic material with little internal friction. On the other hand the formation of the central uplift requires a fluid-like behavior of the target material (Melosh and Ivanov, 1999). This leads to the model of acoustic fluidization, where the so-called *Bingham fluid* takes the role of the target material. The impact induces a seismic shaking of the rock debris lowering their strength, and making the rock behave like a viscous fluid (Melosh and Gaffney, 1983). This type of rheology has also been found to provide an excellent description of the flow of large masses of rock debris in large rock avalanches (Huppert and Brian Dade, 1998).

5.2.3 Transition between Simple and Complex Craters

At a certain diameter threshold the transition between simple to complex craters takes place. This transition diameter is well determined: the transition occurs on the Moon at about 15 km in diameter (Pike, 1976), on Mercury and Mars at about 7 km (Croft, 1985), and the value for Venus at about 4 km was given by Schenk and Sharpton, 1992.

Melosh and Ivanov, 1999 figured out, that the diameter range seems to be dependent to $1/g$ (g is the surface gravity).

5.2.4 Timescale of Crater Collapses

Melosh and Ivanov, 1999 gave these values: for an impactor with 1 km in diameter, a velocity of 15 km/s and an 45° angle of injection, the first stage lasts for about **0.1 seconds**. For craters with diameters in the range from 10 to 100 km the viscous relaxation time is in the range of $\mathbf{10^9}$ **to** $\mathbf{10^{10}}$ **years**.

6 Polygonal Impact Craters (PICs)

6.1 Definition of Polygonal Impact Craters

The definition of PICs according to the proposal of Aittola et al., 2007 is given as:

> *"A Polygonal Impact Crater (PIC) is a crater whose shape in plane view is more or less angular instead of being circular or ellipsoidal, and their rims are composed of at least two straight segments".*

Polygonal impact craters are found on many bodies in the Solar System: On the inner planets and the Moon, on the several moons of the outer planets, e.g. Mimas and Iapetus, and on some of the asteroids, for instance Mathilde and Eros (see Figure 6.1 and 6.2). An occurrence on bodies of the Kuiper belt is likely but unproven.

Among the entire impact crater population on Mars, Venus, and the Moon polygonal impact craters make up ∼10-15 % (Aittola et al., 2010). On Mercury a current study found a fraction of 11 % (Weihs et al., 2012).

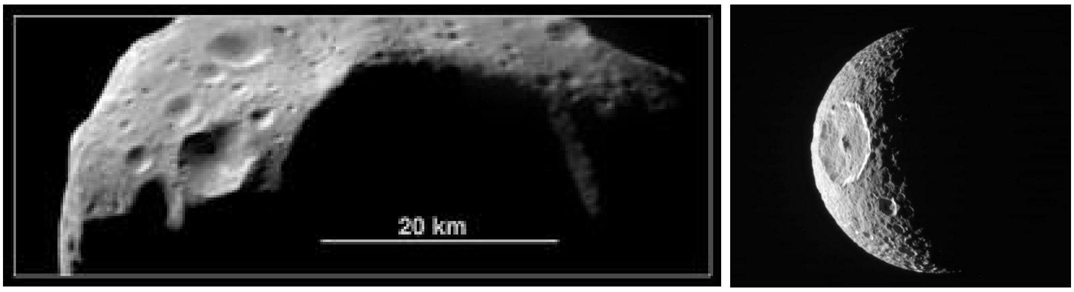

Figure 6.1: Examples of PICs: Asteroid Mathilde, Saturn-moon Mimas (NASA/JPL).

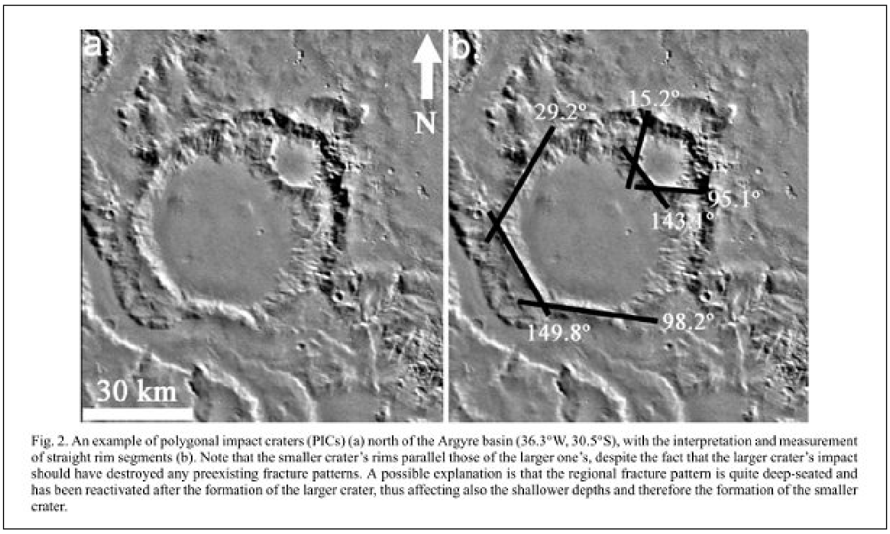

Figure 6.2: Example of a PIC on Mars (Öhman et al., 2006).

6.2 Models for the Formation of Polygonal Impact Craters

> "The polygonal shape is established when the crater forms, and a subsequent crater degradation does not have a significant effect on its shape" (Aittola et al., 2010).

Thus the influence of the geologic structure on the crater shape, especially on zones of structural weakness (corresponding to minor density), operates according to the mechanism of forming PICs out of simple craters and complex craters.

6.2.1 Model 1: Formation of the simple PICs during the Crater Excavation Stage

In this model the target structure becomes dominating near the end of the excavation phase and so the polygonal shape of the crater originates already from this stage.

> *'Excavation of the crater cavity proceeds preferentially along directions of crustal weakness. The cavity is enlarged in directions parallel to the trends of crustal structure'* (Eppler et al., 1983).

Poelchau et al., 2009 presented a more detailed view on how a square-shaped morphology actually forms, demonstrated by the example of the Meteor Crater, Arizona. A pre-impact fracture set was forming the current visible square-shaped crater (see Figure 6.3).

Figure 6.3: Example of a simple PIC: Meteor Crater, Earth (IAU/USGS/NASA-Planetary-Database, 2013).

6.2.2 Model 2: Formation of the complex PICs during the Crater Modification Stage

The gravity collapse in the modification stage results in uplifting the crater floor and in addition to, a sliding of the walls.

> *"The collapse along the fracture planes is taking place in the modification stage, walls fail and slumps develop along trends of structural weakness of the target"* (Eppler et al., 1983).

Crater Mead on Venus (see Figure 6.4) serves as an example of a complex PIC with central peak and terraced rims.

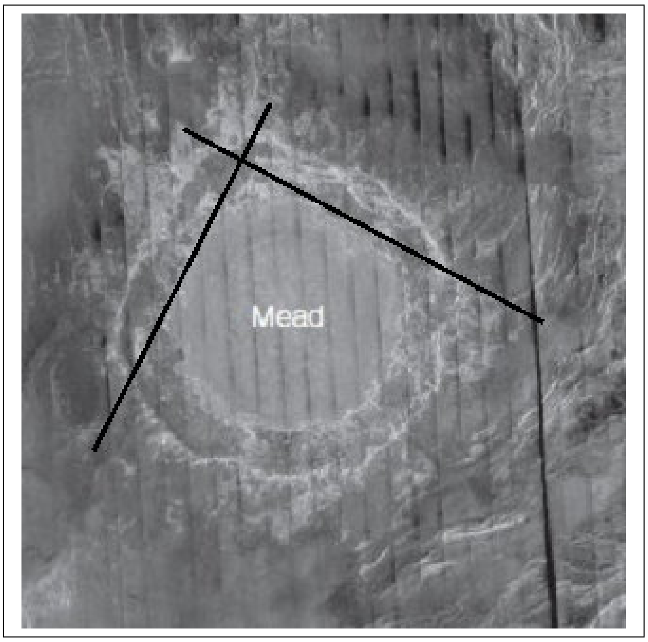

Figure 6.4: Example of a complex PIC: Crater Mead, the largest impact crater on Venus with an diameter of 270 km (IAU/USGS/NASA-Planetary-Database, 2013).

7 The Relative Age of Venusian Impact Craters

7.1 Global Stratigraphic Model of the Venusian Surface

Stratigraphy is based on the principle of superposition and shows a relative time sequence for single forms of landscapes like highlands, tesserae, plains and other features. A practical method used is to monitor the borders of geological subunits, where different types of terrain are meeting. If for instance a lava stream is covering a plain with wrinkle ridges, than it is clear that the plain has to be older than the lava stream. In this way a time sequence can be constructed and rectified in different places on the planet.

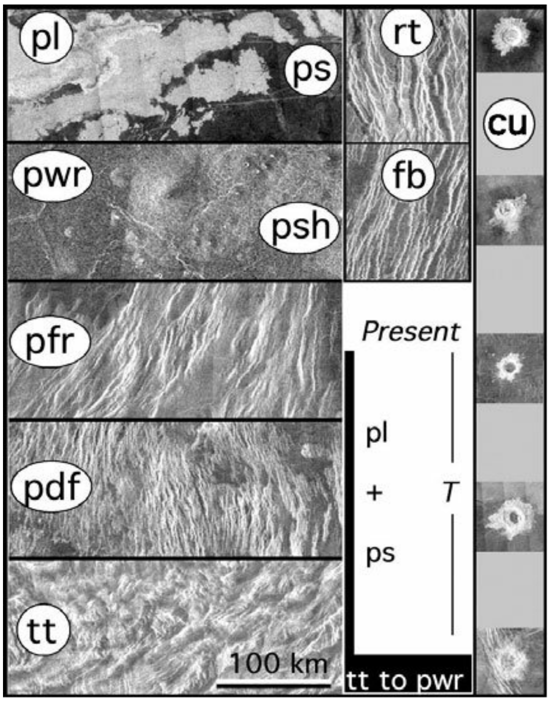

Figure 7.1: Radar images of Magellan of geologic units are arranged in order of a global stratigraphic model of the Venusian history (Basilevsky and Head, 2002a).

Figure 7.1 demonstrates the current model of Basilevsky and Head, 2002a and is showing a typical age sequence of geological units (from older to younger units), identified on the principles of superposition. The model supposes that these local layers reflect a global sequence of the geological events, suggesting planet-wide global synchronous episodes of compression and expansion. According to Basilevsky and Head, 2002a the stratigraphical age sequence of geological units in Figure 7.1 is sorted in order of increasing time:

- (pl) and (ps) - lobate and smooth plains
- (pwr) and (psh) - plains with wrinkle ridges and shield plains
- (pfr) - fractured and ridged plains forming ridge belts
- (pdf) and (tt) - densely fractured plains and tessera terrain

- (rt) and (fb) - structural units corresponding to younger and older rift zones
- (cu) - impact craters are losing their associated dark halos with time
- T is the mean global surface age of Venus estimated to lie within ∼500-750 Myr.

The rapid decrease in the rate of volcanic activity after the emplacement of the plains with wrinkle ridges (pwr) is demonstrated inside the box of Figure 7.1 (Basilevsky and Head, 2002a).

7.2 Determining the Relative Age of Venusian Impact Craters

7.2.1 Stratigraphic Definitions

Some definitions used in this study:

- **Regional plains**: the most widespread plains on Venus cover up to 80 % of the total surface area. Typically they are deformed by wrinkle ridges (Basilevsky and Head, 2000). The term 'regional plains' is used by many authors, e.g. McGill, 2004 and combines plains with wrinkle ridges and shield plains, whereby both types of plains are of volcanic origin (Basilevsky and Head, 2006).
- **wrinkle ridge (WR)**: wrinkle ridges are the result of a modest compressional deformation of plains that led to ∼1-3 % shortening and are characterized by gently rising bumps some km wide but 100-200 km long (Watters, 1988; McGill, 1993; Bilotti and Suppe, 1999).

7.2.2 Known Relative Ages of selected Geological Units

Some values of the mean relative age (see Table 7.1) were estimated by different authors (Schaber et al., 1992; Phillips et al., 1992; Strom et al., 1992; McKinnon et al., 1997). These estimated values agree with the global stratigraphic model (see Figure 7.1), which means that **tessera terrains** are the oldest geological unit, **regional plains** were formed close to T [a], and **lobate plains** and **major rifts** are relatively young (Basilevsky and Head, 2006).

Table 7.1: Known Relative Age of selected Geological Units on Venus. T is the mean absolute surface age, estimated around ∼500-750 Myr (Ivanov and Basilevsky, 1993; Price and Suppe, 1994; Namiki and Solomon, 1994; Izenberg and Arvidson, 1994).

Geological Unit	Relative Age	Source
tessera terrain	(1.47 ± 0.46) T	(Ivanov and Basilevsky, 1993)
regional plains	(1.11 ± 0.09) T	(Price and Suppe, 1994)
large volcanoes (mostly part of lobate plains)	(0.26 ± 0.16) T	(Price and Suppe, 1994)
prominent lava-flow fields (another part of lobate plains)	(0.46 ± 0.33) T	(Price and Suppe, 1994)
major rift zones (mostly rifted terrain unit)	$(0.27 \pm$ T	(Price and Suppe, 1994)
large volcanoes	(0.45 ± 0.1) T	(Namiki and Solomon, 1994)
craters with dark parabolas	< 0.1 T	(Izenberg and Arvidson, 1994)
craters with non-parabolic halos	~ 0.1 to 0.5 T	(Izenberg and Arvidson, 1994)
craters with partial halo and no halo	> 0.5 T	(Izenberg and Arvidson, 1994)

7.2.3 Estimating the Relative Age of Venusian Impact Craters

The number of impact craters on Venus is rather small, about 900, just enough to estimate the absolute mean global surface age of this planet and the mean relative age of a few geological

[a] T is the mean global age of the Venusian surface, estimated around ∼500-750 Myr.

units such as tessera terrain, plains or populations of large volcanoes, but not enough to date individual geologic structures (Ivanov and Basilevsky, 1993; Schaber et al., 1992; Phillips et al., 1992; Strom et al., 1992; Zahnle and McKinnon, 1997). For these reasons there is only the opportunity left to approximately estimate the age of individual impact craters in relation to their neighboring structures.

Basilevsky and Head, 2006 developed a system to study Magellan images of impact craters and their superposition on regional plains, which dominate the surface and typically are deformed by wrinkle ridges, and mostly have radar-dark halos. Under the assumption that the cratering rate was constant during the time interval considered, the approach to the relative age affords an especial technique:

> *"If one finds that of n craters superposed on some unit, m craters are affected by some geologic process (e.g., fracturing), this means that this process occurred within the time interval, which is the m/n fraction of the unit age"* (Basilevsky and Head, 2006).

7.2.3.1 Impact Craters and Regional Plains with Wrinkle Ridges

Basilevsky and Head, 2006 analyzed the images of impact craters considering the following options:

- if a crater's ejecta superpose on regional plains with wrinkle ridges, than the crater is younger than plains with wrinkle ridges (**pre-WR**).
- if a crater's rim or ejecta is deformed by regional plains with wrinkle ridges, than the crater is older than plains with wrinkle ridges (**pre-WR**).

Basilevsky and Head, 2006 demonstrated these age relations found between the regional plains, the wrinkle ridges deforming them, and the impact craters for the example of crater Caccini (see Figure 7.2).

McGill (2004) found in his study that the superpositions were hardly to be recognized for small craters up to 30 km. For this reason Basilevsky and Head, 2006 decided to start their observations from craters $\geq$30 km in diameter.

7.2.3.2 Impact Craters with associated Dark Halos

Radar-dark halos often are associated with Venusian impact craters surrounding the craters' ejecta. Probably these halos are created by the impact of hot air accompanying the projectile. The degree of preservation of the dark halos gives some clues to the age of the craters (Ivanov and Basilevsky, 1993; Strom et al., 1992; Herrick and Phillips, 1994b; Izenberg and Arvidson, 1994). According to Basilevsky and Head, 2002b the craters can be classified into four types (see Figure 7.3):

- craters with dark parabolas (DP).
- with clear dark halo (CH).
- with faint dark halo (FH).
- with no dark halo (NH).

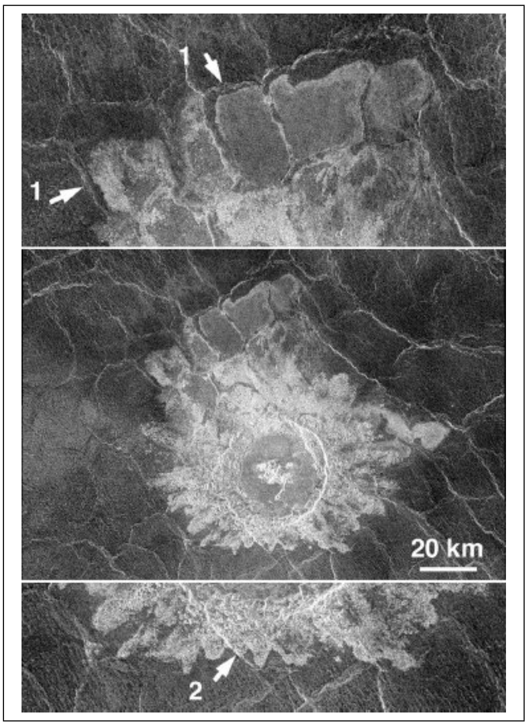

Figure 7.2: Crater Caccini, 17.43° N, 170.43 ° E, D = 38 km, superposed on regional plains and on wrinkle ridges, which control the distribution of crater ejecta outflows (arrows 1). Facies of ejecta maybe are locally controlled by wrinkle ridges (arrow 2) (Basilevsky and Head, 2006).

Izenberg and Arvidson, 1994 considered a slightly different classification as an aging sequence in relation to T [a]. From the percentages of craters Izenberg and Arvidson, 1994 derived the ages as:

- the age of craters with dark parabolas is smaller than ∼0.1 T [a] .
- the age of craters with non-parabolic halos is ∼0.1 T - 0.5 T [a] .
- and the age of craters with a partial halo and no halo is >0.5 T [a] .

(Schaber et al., 1992; Phillips et al., 1992; Strom et al., 1992; McKinnon et al., 1997). For a graphical image of the types of radar-dark halos versus age see Figure 7.4.

7.3 The Relative Age of Impact Craters

Basilevsky and Head (2006) found that among the population of 146 craters on Venus with a diameter ≥30 km which are superposed on wrinkle-ridged regional plains, 10 craters are predating the wrinkle ridges (pre-WR), 93 craters are postdating the wrinkle ridges (post-WR), and 43 craters are ambiguous cases.

The results of McGill (2004) for craters of all sizes, but for only 1/3 of the surface of Venus, gave a similar estimate.

One of the latest papers concerning this topic contains a detailed table of age correlations for the Thetis Regio (see Figure 7.5) (Guseva et al., 2013).

[a] T is the mean global age of the Venusian surface, estimated around ∼500-750 Myr.

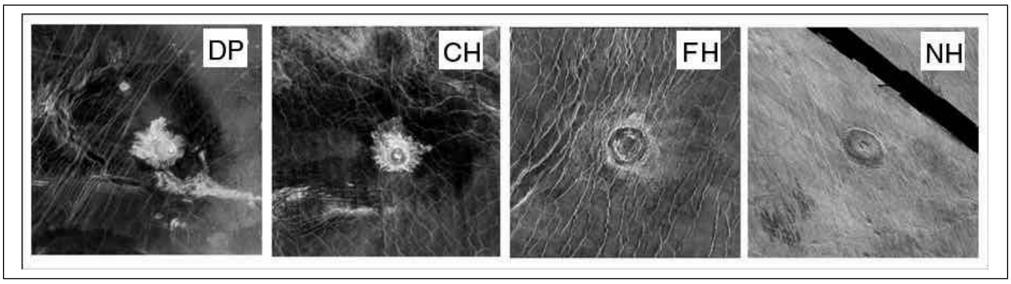

Figure 7.3: Types of crater with radar-dark deposits: (DP) - craters with dark parabolas (CH) - with clear dark halo , (FH) - with faint dark halo, and (NH) - with no dark halo (Basilevsky and Head, 2002b).

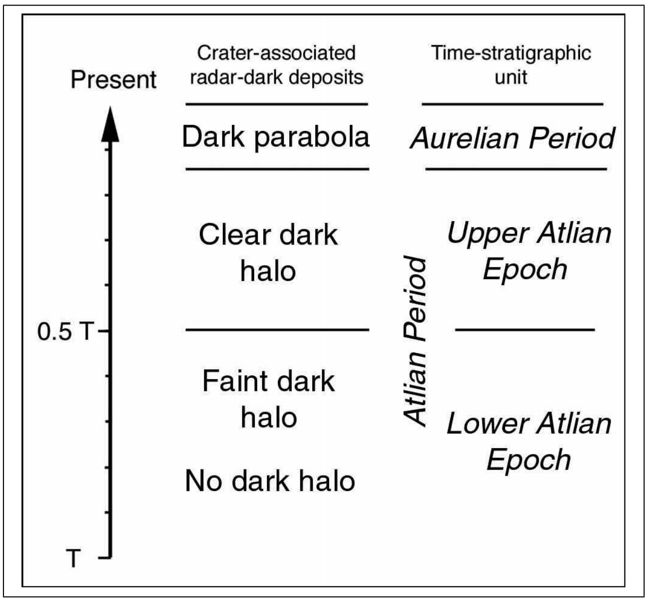

Figure 7.4: Types of crater with radar-dark deposits and corresponding time-stratigraphic units (age sequence from young to older): (DP) - (CH) - (FH) - (NH) (Basilevsky and Head, 2002b).

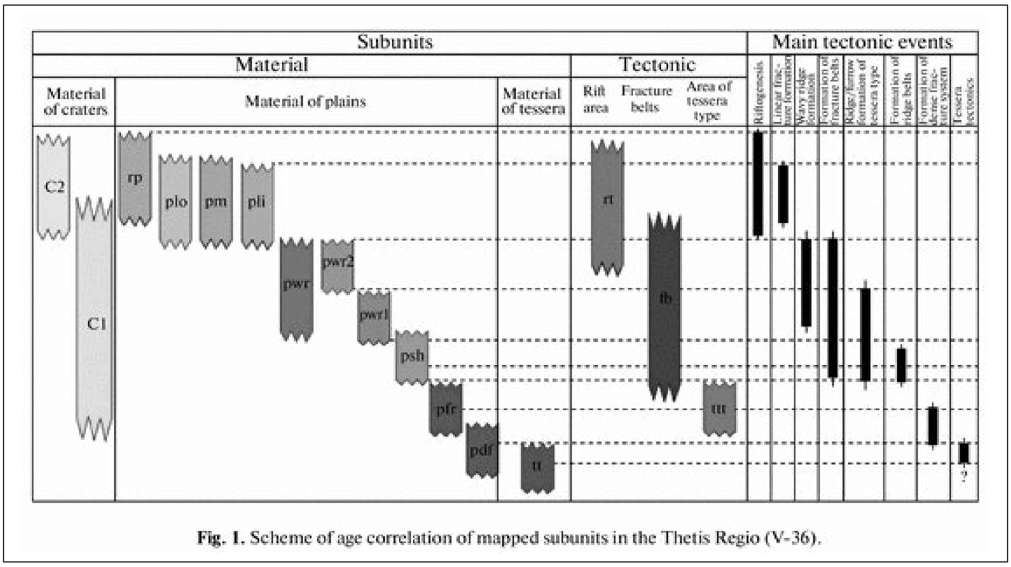

Figure 7.5: Scheme of age correlation of mapped subunits in the Thetis Regio (V36) (Guseva et al., 2013).

8 Determining the Relative Age of Venusian PICs

8.1 Procedure to Estimate the Relative Age

In chapter 7.3 the methods to determine the relative age of Venusian impact craters were discussed. This technique of Basilevsky and Head, 2006 is now applied to Venusian polygonal impact craters (PICs).

For the estimation of the relative age of polygonal impact craters the following scheme was used:

1. Selection of the impact crater database.
2. Selection of PICs to be examined.
3. Screening of the selected images of PICs.

8.1.1 Selection of Venus Impact Crater Database

Two general databases for Venusian impact craters are in use - one compiled by Herrick et al., 1997 and another one by Schaber et al., 1992. In this study both sources were applied, excel-listings from Herrick et al., 1997 and images from USGS Astrogeology Branch web site (url: http://astrogeology.usgs.gov).

- The database 'Release 3 of the Venus Crater Database' was compiled by Robert Herrick and later updated by Herrick et al., 1997. This is the 3rd release with the comfort of having the choice of several file formats like Excel, or tab-delimited text (url: http://www.lpi.usra.edu/resources/vc/vchome.html). Many people have made inputs into this database at one time or another.
- Another general database of craters was prepared by Schaber et al., 1992. A continuously updated version of that database can be found at the USGS Astrogeology Branch web site (url: http://astrogeology.usgs.gov). All images from mission Magellan are available here, including maps and other useful material.

8.1.2 Selection of PICs

The task of the study was to find PICs which can be set in relation to plains with wrinkle ridges, in order to estimate the age of the craters in relation to these plains. The methods used were described in chapter 7.3.

McGill, 2004 demonstrated that the percentage of impact craters superposed on regional plains was strictly dependent on the size of the craters, with a high fraction of ambiguous cases at small sizes (about 82 %) and less than 40 % at diameters of $\geq$30 km. The selection according to crater size has the advantage, to be independent of the local geology, because the crater size is only determined by the projectile mass and the impacting velocity (cf. Formula 8.2).

$$D_{tc} \approx \left(\frac{\rho_p}{\rho_t}\right)^{1/3} L^{0.78} v_i^{0.44} g^{-0.22} sin^{1/3}\theta \tag{8.1}$$

$$D \approx \frac{D_{tc}^{1.13}}{D_{sc}^{0.13}}, \tag{8.2}$$

where D_{tc} is the diameter of the transient crater, ρ_p and ρ_t are the densities of the projectile and the target, g is the surface gravity, L is the projectile diameter, v_i is the impact velocity , θ is the angle of impact from the horizontal direction, and D_{sc} is the diameter where the transition from simple to complex craters takes place (in SI units!) (Basilevsky and Head, 2006).

In ambiguous cases it is impossible to decide whether craters superpose on plains or inverse. According to the papers of McGill, 2004 and Basilevsky and Head, 2006 , we reduced the number of ambiguous cases by selecting polygonal impact craters with a diameter ≥30 km.

The selection of PICs was based on a list of 121 polygonal impact craters on Venus published by Öhman in his PhD-thesis (Öhman, 2009). The complete list of PICs on Venus is given in Appendix Table A.2.

The selection was carried out for PICs ≥30 km in diameter and yielded 22 PICs, the corresponding list is to be seen in Table 8.1.

Statistical analysis using Table 8.1 resulted some relations:

- morphological class (Class): 75 % central peak; and 25 % multiple peaks + peak rings.
- terrain type that crater lies on (Terrain-Type): 68 % undistinguished plains.
- tectonic deformation of crater by exterior processes (Deformed): 86 % no deformation.
- degradation state as defined in Basilevsky et al., 1987: (Degraded): 91 % pristine, apparently intact ejecta deposits; 9 % degraded, small amount of ejecta.

According to these results most of the selected PICs have central peaks, are surrounded by undistinguished plains, suffer no deformation by exterior processes, and are of pristine degradation state.

The distribution of all PICs and the selected PICs with a diameter ≥30 km on the Venusian surface is given in Figure 8.1.

8.1.3 Screening of the Selected Crater Images

In our analysis of the selected 22 craters ≥30 km in diameter we had to identify the superposition of a crater on regional plains and on the wrinkle ridges deforming them, using the classification schema according to the paper of Basilevsky and Head, 2006:

- craters' ejecta or rims are deformed by wrinkle ridges (pre-WR) if
  - ejecta outflows are locally affected by wrinkle ridges.
  - wrinkle ridges on crater floors, and these ridges look similar to wrinkle ridges in the surrounding regional plains.
  - radar-dark floors inside of impact craters on Venus are probably the result of volcanism after the impact, whereas radar-bright floored craters are considered to be pristine.
- craters are superposed on wrinkle ridges (post-WR) if:
  - craters are being superposed on regional plains.
- ambiguous cases.

Table 8.1: Selected PICs ≥30 km in diameter sorted according to ascending diameters. Legend: (Class): morphological class - (1) bowl-shaped; (2) knobby base, (3) central peak, (4) multiple peaks, (5) peak rings, (6) multiple rings, and (0) indistinguishable flat-floored feature; (Terrain-Type): terrain type that crater lies on - (p) undistinguished plains, (pf) fractured plains, (lp) Lakshmi Planum, (t) tessera and mountain belts, (c) corona, (v) volcanic regions, (r) ridge belt and (ri) rift ; (Deformed): tectonic deformation of crater by exterior processes – (y) yes, (n) no, (m) maybe; (Degraded): degradation state as defined in Basilevsky et al. (1987) - (1) pristine, apparently intact ejecta deposits, (2) Degraded, small amount of ejecta; and (3) highly degraded; modified after (Herrick et al., 1997).

Crater Name	**Diameter**	**Latitude**	**Longitude**	**Quad**	**Class**	**Terrain Type**	**Deformed**	**Degraded**
Hwangcini	30.2	6.3	141.8	v24	3	p	n	1
Vacarescu	31.5	-63.0	199.8	v59	3	p	n	1
Mu Guiying	32.3	41.2	81.0	v10	4	p	n	1
Grimke	34.8	17.2	215.3	v27	3	pf	y	1
Bradstreet	36.0	16.5	47.7	v21	3	v	m	1
Mowatt	38.4	-14.6	292.3	v41	3	p	n	1
Agrippina	38.6	-33.2	65.7	v46	3	p	n	1
Howe	38.6	-45.7	174.8	v49	3	p	n	1
Carson	38.8	-24.2	344.1	v43	3	p	n	1
Uvaysi	38.9	2.3	198.3	v26	3	v	n	2
Ban Zhao	39.0	17.1	147.0	v24	3	p	n	1
Phryne	39.4	-46.2	314.7	v54	3	p	n	1
Agnesi	42.4	-39.4	37.7	v45	4	p	n	1
Rhys	44.0	8.6	298.8	v29	3	p	n	1
Austen	45.1	-25.0	168.4	v37/v49	4	ri	n	1
Marsh	47.7	-63.6	46.6	v56	4	p	n	1
de Beauvoir	52.5	2.0	96.1	v23	5	t	y	2
Vigee Lebrun	57.8	17.3	141.4	v24	4	r	n	1
Andreianova	66.1	-3.0	68.8	v34	6	t	n	1
Henie	70.4	-51.9	146.0	v58	4	p	n	1
Sayers	98.0	-67.5	229.8	v59	5	p	n	1
Mead	270.0	12.5	57.2	v21	6	p	n	1

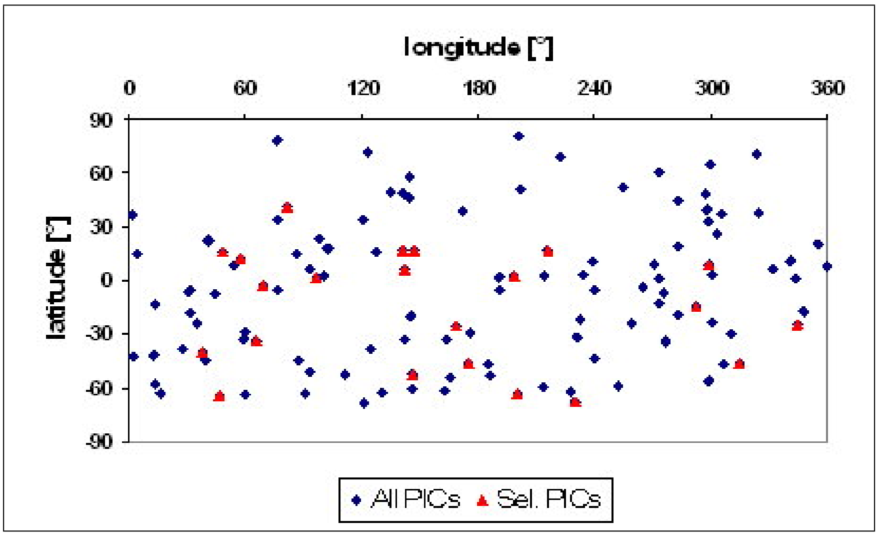

Figure 8.1: Distribution of all PICs and the selected PICs with a diameter ≥30 km on the surface of Venus.

9 Results

9.1 Selected and Screened PICs

In the present study 22 PICs with diameters ≥30 km were selected and screened using the methods described in chapter 7.3. The results of the screening are given in Table 9.1.

Table 9.1: List of the 22 selected PICs ≥ 30 km in diameter on Venus, using the crater database of Herrick (1997), and sorted according to the diameters.
Legend (after (Basilevsky and Head, 2006)): pre/post-WR (post = craters are younger than the plains with wrinkle ridges (post-WR), pre = examples are older than plains with wrinkle ridges (pre-WR), ambig = ambiguous) ; Dark Halo: DP - dark parabolas, CH - clear dark halo, FH - faint dark halo, NH - no dark halo.

Crater Name	**Dia-meter**	**Lati-tude**	**Longi-tude**	**Quad**	**pre /pst WR**	**Dark Halo**	**Surrounding Terrain**
Hwangcini	30.2	6.3	141.8	v24	post	CH	Aphrodite Terra
Vacarescu	31.5	-63.0	199.8	v59	post	NH	Nsomeka Planitia
Mu Guiying	32.3	41.2	81.0	v10	post	FH	Tellus Tessera
Grimke	34.8	17.2	215.3	v27	post	NH	Ulfrun Regio
Bradstreet	36.0	16.5	47.7	v21	pre	NH	Eistla Regio
Mowatt	38.4	-14.6	292.3	v41	post	CH	Dzerassa Planitia
Agrippina	38.6	-33.2	65.7	v46	post	FH	Aino Planitia
Howe	38.6	-45.7	174.8	v49	post	NH	Nsomeka Planitia
Carson	38.8	-24.2	344.1	v43	post	DP	Lavinia Planitia
Uvaysi	38.9	2.3	198.3	v26	pre	NH	Atla Regio
Ban Zhao	39.0	17.1	147.0	v24	post	DP	Llorona Planitia
Phryne	39.4	-46.2	314.7	v54	post	NH	Dione Regio
Agnesi	42.4	-39.4	37.7	v45	post	DP	Fonucho Planitia
Rhys	44.0	8.6	298.8	v29	ambig	NH	Undine Planitia
Austen	45.1	-25.0	168.4	v37/v49	pre	NH	Aphrodite Terra
Marsh	47.7	-63.6	46.6	v56	post	FH	Mugazo Planitia
de Beauvoir	52.5	2.0	96.1	v23	pre	NH	Ovda Regio
Vigee Lebrun	57.8	17.3	141.4	v24	ambig	NH	Aphrodite Terra
Andreianova	66.1	-3.0	68.8	v34	pre	NH	Manotium tessera
Henie	70.4	-51.9	146.0	v58	post	FH	Imapinua Planitia
Sayers	98.0	-67.5	229.8	v59	post	NH	Nuptadi Planitia
Mead	270.0	12.5	57.2	v21	ambig	FH	Eistla Regio

9.2 The Correlation of the Relative Age of PICs with the pre/post-WR Status

The determination of the crater status pre-WR or post-WR required a detailed analysis. As mentioned above, post-WR means craters are younger than the plain with wrinkle ridges, pre-

WR craters are older than the plain with wrinkle ridges, ambiguous cases cannot be decided. The resulting crater states are shown in Table 9.2.

Table 9.2: Numbers and Percentages of the Craters according to the Age Relations to Plains with Wrinkle Ridges (WR). Legend: pre/post-WR: (pre) - craters are older than plains with wrinkle ridges, (post) - craters are younger than the plains with wrinkle ridges, (ambig) - ambiguous state; Number: number of crater's states; Percent: percentage of crater' states.

pre/post WR	**Number**	**Percent**
post-WR	14	63.7
pre-WR	5	22.7
ambiguous	3	13.6
sum	22	

9.2.1 Calculation of the Ratios of the Crater's States

According to the method of Basilevsky and Head, 2006 thoroughly described in chapter 7.3 we built the resulting ratios of the numbers:

- unambiguous cases only: $\frac{number(pre-WR)}{number(post-WR)}$ $\sim$*0.35* ,
- if ambiguous craters are considered as pre-WR: $\frac{number((pre+ambiguous)-WR)}{number(post-WR)}$ $\sim$*0.57* ,
- if ambiguous craters are considered as post-WR: $\frac{number(pre-WR)}{number((post+ambiguous)-WR)}$ $\sim$*0.29* .

This first calculation showed a range of ratios from 0.29 to 0.57, with a mean value of 0.35.

9.2.2 Calculation of the Relative Age

Basilevsky and Head, 2006 found for plains with wrinkle ridges a ratio of $\sim$*0.1*, which means that the relative age of the plains with wrinkle ridges is $\sim$*0.1 T* [a] younger than T [a]. In this way a relative age of the plains with wrinkle ridges of *0.9 T* [a] was yielded.

In a next step the relative age for PICs in relation to the plains with wrinkle ridges were calculated.

Finally an analogous calculation yielded for the difference between the fraction of T [a] computed by Basilevsky and Head, 2006 for plains with wrinkle ridges and our calculated values:

- unambiguous cases only: *0.9 T - 0.35 T = 0.55 T* [a] ,
- if ambiguous craters are considered as pre-WR: *0.9 T - 0.57 T = 0.33 T* [a] ,
- if ambiguous craters are considered as post-WR: *0.9 T - 0.29 T = 0.61 T* [a].

with *0.9 T* [a] is the value for the plains with wrinkle ridges given by Basilevsky and Head (2006).

This calculation resulted in a range of relative ages of PICs on Venus from ∼0.3 T [a] to ∼0.6 T [a].

[a] T is the mean global age of the Venusian surface, estimated around ∼500-750 Myr.

9.3 The Correlation of the Relative Age of PICs with the Abundance of Dark Halos

To check the correctness of the estimation, an alternative method to achieve the value for the relative age of PICs was used - the abundance of radar-dark halos. These radar-dark halos are often observed in association with impact craters on Venus. Several studies on these objects have demonstrated that their existence and their morphology can be seen as a measurement for their age (Ivanov and Basilevsky, 1993; Basilevsky and Head, 2002b; Strom et al., 1992; Herrick and Phillips, 1994b; Izenberg and Arvidson, 1994).

Basilevsky and Head, 2002b found, that the sequence DP-CH-FH-NH (that means Dark Parabolas - Clear dark Halos - Faint dark Halos - No dark Halos) is an evolutionary sequence:

- DP craters are younger than *0.1 - 0.15 T* [a].
- CH craters between *0.1 - 0.15 T and 0.5 T* [a].
- FH and NH craters between *0.5 T and 1 T* [a].

Table 9.3 presents the abundance of the dark crater types versus the numbers of the PICs' states.

Table 9.3: Polygonal Impact Craters Superposed on Regional Plains Distributed within the Dark Halo Categories DP, CH, FH, NH (Dark parabolas, clear dark halos, faint dark halos, no dark halos).

Dark Halos	**All PICs**		**Post-WR PICs**		**Pre-WR PICs**		**Ambiguous PICs**	
	Number	**Percent**	**Number**	**Percent**	**Number**	**Percent**	**Number**	**Percent**
DP	3	13.6	3	21.4	0	0.0	0	0.0
CH	2	9.1	2	14.3	0	0.0	0	0.0
FH	5	22.7	4	28.6	0	0.0	1	33.3
NH	12	54.5	5	35.7	5	35.7	2	66.7
sum	22		14		5		3	

9.4 Conclusions

Detailed analysis of the crater status (pre-WR or post-WR or ambiguous) yielded the results shown in Table 9.2 In some cases the results of either Basilevsky and Head, 2006 or McGill, 2004 were considered.

On the basis of this analysis the relative age for PICs in relation to plains with wrinkle ridges was calculated and resulted in a range between ∼0.33 T [a] and ∼0.61 T [a], and in a mean value of ∼0.55 T [a].

According to the superpositions of craters and plains with wrinkle ridges, the relative age of PICs on Venus shows a range between 0.33 T [a]and 0.61 T [a].

Additionally the known age sequence of radar-dark halos DP-CH-FH-NH (that means dark parabolas - clear dark halos - faint dark halos - no dark halos) after (2002) Basilevsky and Head, 2002b was used to date PICs in terms of fractions of T [a]. Basilevsky and Head, 2002b found that DP-craters are younger than *0.1 - 0.15 T* [a], CH-craters between *0.1 T* and *0.5 T* [a], and FH- and NH- craters between *0.5 and 1 T* [a] (cf. Table 9.4).

[a] T is the mean global age of the Venusian surface, estimated around ∼500-750 Myr.

Table 9.4: Polygonal Impact Craters Superposed on Regional Plains Distributed within the Dark Halo Categories DP, CH, FH, NH (Dark parabolas, clear dark halos, faint dark halos, no dark halos).

	Dark Halos	**All PICs**	
Dark Halos	**Relative Age**	**Number**	**Percent**
DP	< 0.1 T	3	13.6
CH	0.1 - 0.5T	2	9.1
FH	> 0.5 T	5	22.7
NH	> 0.5 T	12	54.5
sum		22	

More than 86 % of the PICs lie in the range of the dark halos types CH, FH, and NH (clear dark halos , faint dark halos, no dark halos) and the relative age of these dark halos covers a range from 0.1 T [a] to more than 0.5 T [a]. This means that the range of the relative age of PICs determined with both methods matches well.

According to the abundance of radar-dark halos, the relative age of PICs on Venus shows a range between ∼0.1 T and ≥0.5 T [a]

In the combination of both results the **final result** was achieved:

The mean relative age of PICs on Venus shows a range between ∼0.33 T [a] and ∼0.61 T [a]

9.5 Images of the selected PICs

The images of all selected and screened 22 PICs are given in Appendix A.3.

[a] T is the mean global age of the Venusian surface, estimated around ∼500-750 Myr.

10 Summary

- In this study the relative age of 22 selected polygonal impact craters (PICs) on Venus were examined.
- A set of PICs ≥30 km in diameter was selected, and the superposition of the craters on regional plains with wrinkle ridges, the deformation of crater rims or ejecta by wrinkle ridges and additionally the abundance of dark halos surrounding the craters was examined.
- Using the methods developed by Basilevsky and Head, 2006 and McGill, 2004 the relative age of PICs on Venus was obtained.
- In the study it was proved that PICs are located in a similar range of relative ages as other impact craters. Only a few craters, mostly situated in tesserae are older than the plains.

The mean relative age of the selected set of PICs on Venus lies in a range from ∼0.33 T [a] to ∼0.61 T [a].

For example if T [a] = 500 Myr, then the mean relative age of the PICs results in about 235 ±70 Myr, that is a range between 165 and 305 Myr.

Figure 10.1 plots the final result of this study - the relative age of polygonal impact craters (PICs) on Venus in comparison to the relative age of several other geological units of the Venusian Surface.

These results can be interpreted as an evidence that the formation of PICs was a distinct phase in the geological history of Venus and that it happened rather at the end of the (last) resurfacing stage.

[a] T is the mean global age of the Venusian surface, estimated around ∼500-750 Myr.

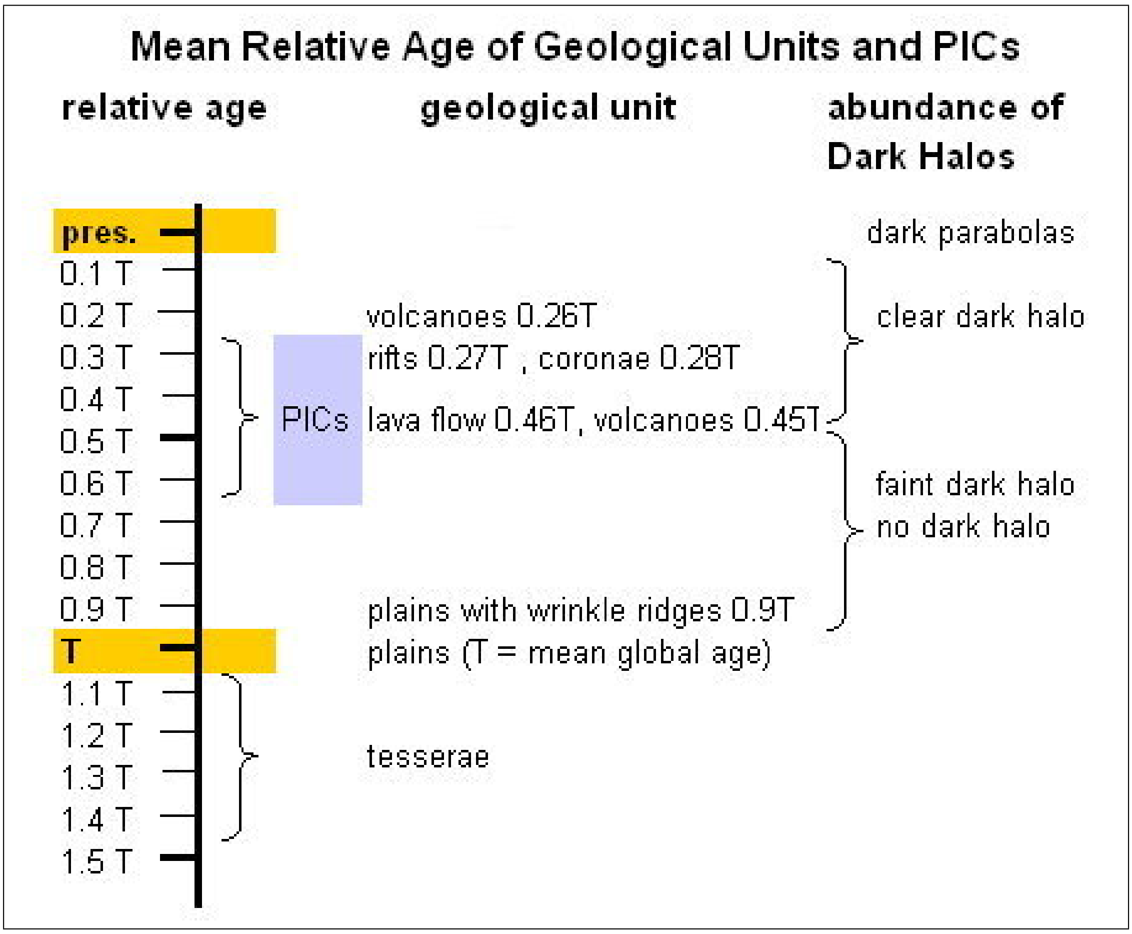

Figure 10.1: Relative Age of Polygonal Impact Craters on Venus and several other Geological Units of the Venusian Surface.
Legend: relative age - the scale is representing fractions of T (T is the mean absolute age of the Venusian surface, estimated to lie within 500 to 750 Myr); geological unit - the relative age of typical units of the surface like tesserae, plains, plains with wrinkle ridges, volcanoes, lava flows, rifts, and coronae; abundance of dark halos - dark parabolas, clear dark halos, faint dark halos, and no dark halos.

A Appendix

A.1 Table of all All Venusian Impact Craters

Table A.1: All Venusian Impact Craters after (Herrick and Phillips, 1994b).

Feature Name	Diameter	Latitude	Longitude
Abigail	18.4	-52.2	111.2
Abika	14.5	-52.5	104.4
Abington	21.7	-47.8	277.7
Abra	7.2	6.2	97.4
Adaiah	18.0	-47.3	253.4
Adamson	27.2	-14.8	29.6
Addams	87.0	-56.2	98.9
Adivar	30.3	8.9	76.2
Adzoba	10.0	12.8	117.0
Aethelflaed	20.0	-18.2	196.6
Afiba	9.5	-47.1	102.7
Afiruwa	5.2	4.3	3.8
Aftenia	7.0	50.0	324.0
Afua	10.0	15.5	124.0
Aglaonice	63.7	-26.4	339.9
Agnesi	42.4	-39.4	37.7
Agoe	6.3	13.1	4.3
Agrippina	38.6	-33.2	65.7
Ahava	10.4	53.6	187.3
Aigul	6.0	38.2	280.4
Ailar	8.2	-15.8	68.4
Aimee	17.0	16.1	127.2
Aisha	10.6	39.3	53.3
Aita	14.0	8.9	270.7
Akeley	23.4	8.0	244.5
Akhmatova	41.4	61.3	307.9
Akiko	17.4	30.6	187.3
Akosua	6.2	-58.6	18.1
Aksentyeva	42.5	-42.0	271.9
Akuba	5.5	9.6	23.0
Alcott	66.0	-59.5	354.4
Alima	10.3	-46.0	229.2
Alimat	13.5	-29.5	205.9
Alina	3.7	8.3	267.8
Alison	14.4	-4.0	165.6
Alma	16.8	-2.4	228.8
Almeida	15.5	46.6	123.3
Altana	6.0	1.4	69.9
Al Taymuriyya	19.0	32.9	336.1
Amalasthuna	15.4	-11.5	342.4
Amalasuntha	15.4	-11.5	342.4
Amanda	12.5	-29.2	94.5
Amaya	34.5	11.3	89.4
Amelia	3.3	8.6	280.5

continued ...

Table A.1: All Venusian Impact Craters after (Herrick and Phillips, 1994b) - continued .

Feature Name	Diameter	Latitude	Longitude
Amenardes	27.9	15.0	54.3
Aminata	9.7	6.6	25.2
Anaxandra	20.4	44.2	162.3
Andami	28.9	-17.5	26.5
Andreianova	66.1	-3.0	68.8
Anicia	38.2	-26.3	31.3
Annia Faustina	23.4	22.1	4.7
Antonina	13.8	28.1	106.8
Anush	12.7	14.9	86.5
Anya	18.1	39.5	297.8
Ariadne	23.6	43.9	360.0
Asmik	19.5	3.9	166.4
Astrid	10.5	-21.4	335.2
Audrey	15.2	23.8	348.1
Aurelia	31.1	20.3	331.8
Austen	45.1	-25.0	168.4
Avene	10.0	40.4	149.4
Avviyar	20.6	-18.0	353.7
Ayana	13.8	-29.2	175.5
Ayashe	6.7	22.7	31.4
Ayisatu	7.0	34.6	5.5
Bachira	7.3	26.5	10.0
Badarzewska	29.6	-22.6	137.2
Bahriyat	5.0	50.3	357.5
Baker	109.0	62.5	40.3
Bakisat	7.4	26.0	356.8
Balch	40.0	29.9	282.9
Ban Zhao	39.0	17.1	147.0
Baranamtarra	25.5	17.9	267.8
Barauka	12.9	10.6	346.3
Barrera	27.0	16.6	109.4
Barrymore	56.6	-52.3	195.7
Barsova	76.0	61.3	223.0
Barto	48.0	45.3	146.3
Barton	52.2	27.4	337.5
Bascom	34.6	-10.4	302.2
Bashkirtseff	36.2	14.7	194.0
Bassi	31.0	-19.0	64.6
Bathsheba	32.3	-15.1	49.5
Batten	65.0	15.2	217.4
Batya	9.3	72.7	235.4
Beecher	40.4	13.0	253.4
Behn	25.4	-32.4	142.0
Bender	39.8	-13.0	327.4
Berggolts	29.5	-63.5	53.0
Bernadette	12.8	-46.6	285.6
Bernhardt	25.3	31.6	84.4
Bernice	12.6	-40.7	14.8
Berta	20.0	62.0	322.0
Bette	7.2	-24.6	347.9
Bickerdyke	36.3	-82.0	171.3
Bineta	10.7	57.3	144.1
Birute	22.3	36.1	32.0
Blackburne	30.5	11.0	183.9
Blanche	12.3	-9.3	157.0
Blixen	20.8	-60.1	145.7

continued ...

Table A.1: All Venusian Impact Craters after (Herrick and Phillips, 1994b) - continued .

Feature Name	Diameter	Latitude	Longitude
Bly	18.7	37.7	305.5
Boivin	20.4	4.3	299.5
Boleyn	70.4	24.4	220.1
Bonnevie	92.2	-36.1	127.0
Bonnin	28.5	-6.3	117.6
Boulanger	71.5	-26.6	99.2
Bourke White	33.6	21.2	147.9
Boyd	22.0	-39.4	221.4
Boye	28.0	-9.6	292.3
Bradstreet	36.0	16.5	47.7
Bridgit	10.0	-45.3	348.9
Brooke	22.9	48.4	296.6
Browning	23.4	28.3	4.9
Bryce	23.9	-62.5	197.0
Buck	21.8	-5.7	349.6
Budevska	18.0	0.5	143.2
Bugoslavskaya	29.9	-23.0	300.4
Caccini	38.1	17.4	170.4
Caitlin	14.7	-65.3	12.0
Caiwenji	22.6	-12.4	287.6
Caldwell	51.0	23.6	112.4
Callas	33.8	2.4	27.0
Callirhoe	33.8	21.2	140.7
Caroline	18.0	6.9	306.3
Carr	31.9	-24.0	295.7
Carreno	57.0	-3.9	16.1
Carson	38.8	-24.2	344.1
Carter	17.5	5.3	67.3
Castro	22.9	3.4	233.9
Cather	24.6	47.1	107.0
Centlivre	28.8	19.1	290.4
Chapelle	22.0	6.4	103.8
Chechek	7.2	-2.6	272.3
Chiyojo	40.2	-47.8	95.7
Chloe	18.6	-7.4	98.6
Cholpon	6.3	40.0	290.0
Christie	23.3	28.3	72.7
Chubado	7.0	45.3	5.6
Clara	3.2	-37.5	235.3
Clementina	4.0	35.9	208.6
Cleopatra	105.0	65.8	7.1
Cline	38.0	-21.8	317.1
Clio	11.4	6.3	333.5
Cochran	100.0	51.9	143.4
Cohn	18.3	-33.3	208.1
Colette	0.0	65.0	322.0
Colleen	13.5	-60.8	162.2
Colonna	28.0	64.7	216.8
Comnena	19.5	1.2	343.7
Conway	49.3	48.3	39.0
Cori	56.1	25.4	72.9
Corinna	19.2	22.9	40.6
Corpman	46.0	0.3	151.8
Cortese	27.7	-11.4	218.4
Cotton	48.1	70.8	300.2
Cunitz	48.6	14.5	350.9

continued ...

Table A.1: All Venusian Impact Craters after (Herrick and Phillips, 1994b) - continued .

Feature Name	Diameter	Latitude	Longitude
Cynthia	15.9	-16.7	347.5
Dado	11.2	-13.9	87.6
Dafina	5.5	28.6	244.1
Danilova	48.8	-26.4	337.2
Danute	12.3	-63.5	56.5
Daphne	15.5	41.3	280.4
Darline	13.0	-19.3	232.6
Dashkova	45.1	78.2	306.5
Datsolalee	17.5	38.3	171.8
de Ayala	19.0	12.4	31.9
de Beausoleil	28.2	-5.0	102.8
de Beauvoir	52.5	2.0	96.1
Deborah	9.7	-37.3	10.6
Defa	8.5	32.2	11.3
Degu	5.5	27.3	289.9
Deken	48.0	47.1	288.5
de Lalande	21.3	20.5	355.0
Deledda	32.0	76.0	127.5
Delilah	18.5	-57.9	250.2
Deloria	31.9	-32.0	97.1
Dena	2.4	-20.7	338.7
Denise	2.0	-14.4	94.7
de Stael	25.0	37.4	324.3
d Este	21.6	-34.3	238.9
Devorah	4.8	-22.5	343.4
Devorguilla	22.9	15.3	4.0
De Witt	20.7	-6.5	275.6
Dheepa	4.7	-21.6	176.3
Dickinson	67.5	74.6	177.2
Dinah	15.6	-62.9	37.1
Dix	63.3	-37.0	329.0
Dolores	12.6	51.4	201.6
Domnika	6.7	18.4	294.3
Doris	14.5	2.3	90.0
Dorothy	8.4	-35.4	11.3
du Chatelet	18.5	21.5	165.0
Duncan	40.3	68.1	291.7
Dunghe	5.5	-56.2	295.3
Durant	21.1	-62.3	227.7
Duse	30.4	-82.5	358.0
Dyasya	7.8	5.1	297.6
Earhart	0.0	72.0	136.0
Edgeworth	29.0	32.2	22.8
Edinger	33.3	-68.8	208.5
Efimova	26.5	81.0	223.0
Eila	9.5	-75.0	94.6
Eileen	16.1	-22.8	232.7
Eini	5.9	-41.6	96.4
Elena	17.6	-18.3	73.4
Elenora	4.5	47.1	6.9
Elizabeth	10.5	59.1	215.4
Ellen	14.6	-22.8	281.3
Elma	10.2	-10.1	91.1
Elza	18.0	-34.4	275.9
Emilia	12.5	-26.5	88.2
Emma	11.8	-13.7	302.3

continued ...

Table A.1: All Venusian Impact Craters after (Herrick and Phillips, 1994b) - continued .

Feature Name	Diameter	Latitude	Longitude
Enid	9.2	16.4	352.1
Erika	10.5	72.0	175.4
Erin	13.6	-47.0	184.8
Erinna	33.8	-78.0	309.1
Erkeley	8.0	43.9	103.3
Ermolova	60.9	60.3	154.4
Erxleben	31.6	-50.9	39.4
Escoda	19.6	18.2	149.5
Esmeralda	9.8	64.4	104.5
Estelle	18.8	1.1	93.7
Esterica	3.6	36.8	3.6
Esther	17.6	19.4	21.8
Eudocia	27.5	-59.1	202.0
Eugenia	6.0	80.6	105.4
Evangeline	16.0	69.6	221.9
Eve	23.0	-32.0	0.1
Evelyn	18.0	-61.2	212.3
Evika	20.3	-5.1	31.4
Ezraela	7.8	57.0	186.8
Faiga	9.6	4.9	170.9
Faina	10.0	71.1	100.7
Farida	18.0	4.8	39.0
Fatima	14.5	-17.8	31.9
Faufau	7.8	18.8	8.3
Fava	9.7	-0.7	87.4
Fazu	6.1	32.4	106.0
Fedorets	57.6	59.7	65.6
Fedosova	24.0	45.0	171.8
Felicia	11.5	-19.8	226.5
Ferber	23.1	26.4	12.9
Fernandez	23.7	76.2	17.2
Ferrier	29.1	15.7	111.3
Feruk	8.3	-64.0	107.6
Festa	35.3	11.5	27.2
Fiona	3.5	5.0	166.6
Firuza	6.0	51.8	108.0
Flagstad	39.2	-54.3	18.9
Florence	10.5	-15.2	85.0
Flutra	6.0	-68.4	112.0
Fossey	30.4	2.0	188.7
Fouquet	47.8	-15.1	203.5
Francesca	17.0	-28.0	57.7
Frank	22.7	-13.1	12.9
Fredegonde	25.2	-50.5	93.3
Frida	21.6	68.2	55.6
Frosya	9.8	29.5	113.4
Fukiko	13.9	-23.1	105.8
Gabriela	17.5	-17.8	240.4
Gahano	4.5	-80.2	77.4
Gail	10.0	-16.1	97.5
Galina	16.8	47.6	307.1
Galindo	23.8	-23.3	258.8
Gautier	59.3	26.3	42.8
Gaze	33.3	17.9	240.2
Gentileschi	20.5	45.2	260.6
Georgina	5.9	-20.4	58.8

continued ...

Table A.1: All Venusian Impact Craters after (Herrick and Phillips, 1994b) - continued .

Feature Name	Diameter	Latitude	Longitude
Gerda	30.0	45.9	91.0
Germain	35.5	-37.9	63.7
Giliani	19.9	-72.9	142.1
Gillian	14.7	-15.2	50.1
Gilmore	21.3	-6.7	132.8
Gina	14.6	78.1	76.5
Giselle	10.4	-11.8	298.0
Glaspell	26.3	-58.4	269.6
Gloria	20.7	68.5	94.2
Godiva	30.7	-56.1	251.6
Goeppert Mayer	33.5	59.7	26.8
Golubkina	28.4	60.3	286.5
Goncharova	30.3	-63.0	97.7
Goppert Mayer	33.5	59.7	26.8
Grace	19.0	-13.8	268.9
Graham	75.0	-6.0	6.0
Grazina	16.5	72.4	337.5
Greenaway	93.0	22.9	145.1
Gregory	18.0	7.1	95.8
Gretchen	20.8	-59.7	212.3
Grey	50.0	-52.4	329.4
Grimke	34.8	17.2	215.3
Guan Daosheng	43.6	-61.1	181.8
Gudrun	13.3	10.6	326.4
Guilbert	25.5	-58.0	13.6
Gulchatay	9.0	20.5	295.5
Gulnara	5.0	-23.7	174.0
Guzel	7.3	-57.6	298.7
Gwynn	32.0	9.7	37.2
Hadisha	8.9	-39.0	97.2
Halima	8.9	28.5	14.6
Halle	21.5	-19.8	145.5
Hamuda	15.8	62.9	2.5
Hanka	5.0	-27.3	114.3
Hannah	19.8	17.9	102.6
Hansberry	26.6	-22.7	324.1
Hapei	4.2	66.1	178.0
Hayashi	43.1	53.8	243.9
Heather	11.5	-6.8	334.1
Heidi	15.2	23.6	350.1
Helga	8.8	-10.4	116.7
Hellman	34.7	4.7	356.3
Heloise	38.0	40.0	51.9
Helvi	12.2	12.4	82.7
Henie	70.4	-51.9	146.0
Hepworth	62.6	5.1	94.7
Higgins	40.0	8.1	241.3
Hilkka	10.3	-69.0	72.0
Himiko	36.6	19.0	124.3
Hiriata	5.0	15.3	23.5
Hiromi	6.0	35.2	287.3
Holiday	27.7	-46.7	12.8
Horner	25.2	23.4	97.7
Howe	38.6	-45.7	174.8
Hsueh T ao	21.0	-52.6	13.8
Hua Mulan	24.0	86.8	337.7

continued ...

Table A.1: All Venusian Impact Craters after (Herrick and Phillips, 1994b) - continued .

Feature Name	Diameter	Latitude	Longitude
Huang Daopo	29.1	-54.2	165.3
Huarei	8.5	15.0	32.3
Hull	47.3	59.4	263.6
Hurston	52.4	-77.6	94.7
Hwangcini	30.2	6.3	141.8
Icheko	5.9	6.6	97.9
Ichikawa	31.4	-61.6	156.3
Ilga	10.8	-12.4	307.3
Imagmi	7.6	-48.4	100.7
Indira	16.6	64.1	289.8
Ines	11.2	-67.1	241.9
Inga	10.0	38.1	226.6
Ingrid	11.5	-12.4	308.9
Inira	16.5	-43.1	239.4
Inkeri	10.1	-28.3	223.9
Iondra	7.9	10.5	286.5
Iraida	6.5	27.8	108.1
Irene	13.6	49.8	134.0
Irina	15.2	35.0	91.2
Irinuca	8.0	51.4	121.9
Irma	9.5	-50.9	122.0
Isabella	175.0	-29.8	204.2
Isako	13.5	-9.0	278.0
Isolde	11.9	-74.5	211.9
Istadoy	5.4	-51.8	132.6
Ivka	14.9	68.2	303.8
Ivne	9.0	-27.0	132.8
Izakay	10.2	-12.3	210.8
Izudyr	6.6	-53.9	135.2
Jaantje	7.8	46.5	123.0
Jacqueline	16.5	-70.1	123.6
Jadwiga	12.7	68.4	91.0
Jalgurik	7.5	-42.3	125.1
Jamila	7.9	45.8	134.8
Jane	10.2	-60.5	304.8
Janice	10.0	87.3	261.9
Janina	9.3	-2.0	135.7
Janyl	5.6	-28.0	138.8
Jasmin	15.1	15.6	61.6
Jeanne	19.4	40.1	331.5
Jennifer	9.6	-4.6	99.8
Jerusha	17.2	-22.0	342.7
Jex Blake	31.6	65.4	169.3
Jhirad	50.2	-16.8	105.6
Jitka	13.0	-61.9	70.9
Jocelyn	14.0	-33.2	276.4
Jodi	10.2	-35.7	68.7
Johanna	15.1	19.5	247.3
Johnson	24.5	51.8	254.6
Joliot Curie	91.1	-1.6	62.4
Josefina	26.0	44.9	32.3
Joshee	37.0	5.5	288.7
Juanita	19.3	-62.8	90.0
Judith	16.6	-29.1	104.5
Julie	13.5	51.0	242.6
Jumaisat	7.5	-15.1	135.6

continued ...

Table A.1: All Venusian Impact Craters after (Herrick and Phillips, 1994b) - continued .

Feature Name	Diameter	Latitude	Longitude
Jutta	7.0	0.0	142.6
Kafutchi	7.1	26.7	16.4
Kahlo	35.6	-59.9	178.9
Kaikilani	19.9	-32.8	163.2
Kaisa	12.0	13.5	293.3
Kala	17.4	1.5	314.4
Kalombo	9.6	-30.5	34.0
Kanik	16.5	-32.5	249.9
Karen	10.5	-12.4	17.7
Karo	7.0	21.9	37.2
Kartini	23.4	57.8	333.0
Kastusha	13.0	-28.6	59.9
Katrya	9.2	-29.5	108.7
Katya	10.5	57.8	285.7
Kauffman	25.5	49.4	27.1
Kavtora	9.8	59.0	23.3
Kelea	24.5	8.9	25.6
Kelila	5.0	52.6	191.8
Kelly	11.2	-4.8	359.2
Kemble	23.6	47.7	14.9
Kenny	52.7	-44.4	271.1
Ketzia	14.6	3.9	300.5
Khadako	7.4	54.2	139.3
Khafiza	7.0	6.0	299.2
Khatun	44.1	40.3	87.2
Khelifa	10.8	-1.5	129.9
Kimitonga	5.0	-25.1	48.3
Kingsley	26.6	-22.6	306.4
Kiris	13.3	20.9	98.8
Kitna	15.3	-28.9	277.3
Klafsky	25.5	-20.7	188.1
Klenova	141.0	78.1	104.5
Kodu	10.5	0.9	338.7
Koidula	67.0	64.2	139.6
Koinyt	11.7	-30.9	293.2
Kollado	5.5	-61.0	53.4
Kollwitz	29.1	25.2	133.6
Konopnicka	20.1	14.5	166.6
Kosi	7.7	-43.9	54.9
Kristina	9.7	-65.2	315.9
Kumba	11.4	26.3	332.7
Kumudu	4.4	61.3	154.1
Kuro	8.8	7.8	57.6
Kyen	5.2	-6.2	64.7
Kylli	13.2	41.1	67.0
Lachappelle	36.8	26.7	336.7
La Fayette	39.6	70.2	107.6
Lagerlof	56.0	81.2	285.2
Landowska	33.0	84.6	74.3
Langtry	50.3	-17.0	155.0
Lara	3.4	-4.2	2.9
Larisa	3.7	-18.5	131.1
Laulani	12.4	-68.2	121.2
Laura	17.2	48.9	141.2
Laurencin	29.8	-15.4	46.5
Lazarus	24.2	-52.9	127.2

continued ...

Table A.1: All Venusian Impact Craters after (Herrick and Phillips, 1994b) - continued .

Feature Name	Diameter	Latitude	Longitude
Leah	12.0	-34.2	187.8
Lebedeva	37.4	45.2	49.8
Lehmann	21.7	-44.1	39.1
Leida	18.8	-23.3	266.6
Leila	18.8	-44.2	86.8
Lena	15.2	39.5	23.0
Lenore	15.5	38.7	292.2
Leona	3.0	-3.1	169.0
Leonard	31.7	-73.8	185.2
Leslie	7.2	-11.2	13.5
Letitia	17.5	34.5	288.7
Leyster	45.8	1.0	260.0
Lhagva	7.9	-75.8	300.1
Lida	20.3	36.6	273.9
Lida	12.5	-29.2	94.5
Lilian	13.5	25.6	336.0
Liliya	15.0	30.2	31.1
Lind	25.8	50.2	355.0
Linda	7.1	-12.4	2.8
Lineta	15.6	-5.0	354.1
Li Qingzhao	22.8	23.7	94.6
Lisa	4.5	29.0	182.0
Liv	11.2	-21.1	303.9
Loan	7.4	28.3	60.0
Lockwood	22.0	-32.9	51.6
Lois	13.5	-17.9	214.7
Lonsdale	43.0	55.6	222.4
Lorelei	15.0	55.7	243.9
Loretta	13.5	-19.7	202.6
Lotta	11.8	51.1	335.9
Lucia	16.0	-62.1	67.8
Lullin	25.1	23.0	81.3
Lu Zhi	8.3	-42.6	303.4
Lydia	15.2	10.7	340.7
Lyon	12.4	-66.5	270.6
Lyuba	12.4	1.6	283.9
Lyudmila	14.1	62.1	329.7
Maa Ling	6.0	-14.7	359.5
MacDonald	17.6	30.0	120.7
Madeleine	16.0	-4.7	293.2
Madina	6.3	22.7	58.0
Mae	7.5	-40.5	345.2
Magda	10.1	67.0	329.7
Magdalena	11.5	-11.2	48.7
Magnani	26.4	58.6	337.2
Mahina	15.4	-2.0	182.2
Makola	16.6	-3.8	106.7
Maltby	36.6	-23.3	119.7
Mamajan	2.0	-65.1	257.3
Mansa	8.1	-33.9	63.4
Manton	20.5	9.3	26.9
Manzolini	41.8	25.6	91.3
Maranda	16.8	4.9	169.7
Marere	6.3	19.6	65.8
Maret	11.7	-33.3	280.2
Margarita	13.0	12.7	9.2

continued ...

Table A.1: All Venusian Impact Craters after (Herrick and Phillips, 1994b) - continued .

Feature Name	Diameter	Latitude	Longitude
Margit	14.0	60.1	273.1
Maria Celeste	97.5	23.4	140.4
Marianne	9.0	9.3	358.0
Marie	14.2	-21.7	232.4
Mariko	12.9	-23.3	132.9
Markham	71.8	-4.1	155.6
Marsh	47.7	-63.6	46.6
Martinez	23.5	-11.7	174.7
Marysya	6.3	53.3	75.1
Marzhan	13.8	-58.9	248.3
Masako	23.8	-30.2	53.2
Masha	16.0	63.0	88.0
Masha	6.4	60.7	88.5
Ma Shouzhen	18.9	-35.7	92.5
Matahina	8.5	-72.3	65.9
Maurea	9.9	-39.5	69.1
Mbul di	6.0	23.8	74.7
Mead	270.0	12.5	57.2
Medhavi	30.4	-19.4	40.6
Megan	15.8	-61.8	130.6
Meitner	149.0	-55.6	321.6
Melanie	12.3	-62.8	144.3
Melanka	9.0	34.4	19.2
Melba	21.8	4.7	193.5
Melina	12.7	-69.9	319.5
Meredith	11.4	-14.5	278.9
Merian	22.2	34.5	76.3
Merit Ptah	16.5	11.4	115.6
Michelle	15.0	-19.6	40.5
Mildred	12.0	-51.7	348.3
Millay	48.0	24.4	111.2
Miovasu	4.5	72.1	99.9
Mirabeau	23.8	1.1	284.3
Miriam	16.5	36.5	48.2
Mona Lisa	79.4	25.6	25.1
Monika	25.5	72.3	122.4
Montagu	20.0	36.9	177.7
Montessori	42.1	59.4	280.0
Montez	21.1	17.9	266.5
Moore	21.1	-30.4	248.4
Morisot	48.0	-61.2	211.3
Mosaido	7.4	17.3	75.2
Moses	28.0	34.6	119.9
Mowatt	38.4	-14.6	292.3
Mu Guiying	32.3	41.2	81.0
Mukhina	24.5	29.5	0.5
Mumtaz Mahal	38.2	30.3	228.4
Munter	32.1	-15.3	39.3
Muriel	20.2	-41.7	12.4
Nadeyka	9.3	-54.8	305.3
Nadia	11.3	-27.9	0.6
Nadine	18.6	7.8	359.1
Nadira	31.4	44.1	201.5
Nakai	4.5	-61.0	286.2
Nalkowska	22.2	28.1	290.0
Nalkuta	6.5	30.1	307.8

continued ...

Table A.1: All Venusian Impact Craters after (Herrick and Phillips, 1994b) - continued .

Feature Name	Diameter	Latitude	Longitude
Namiko	13.0	43.4	56.2
Nana	8.8	49.8	75.4
Nancy	4.4	6.4	272.2
Nanichi	19.0	-44.8	337.8
Naomi	17.5	6.0	70.3
Nastya	12.5	-49.0	275.8
Natalia	10.8	67.1	272.9
Ndella	5.9	-15.9	60.7
Neda	7.7	16.7	313.5
Nedko	8.5	-8.8	317.6
Neeltje	10.0	12.4	124.4
Nelike	6.3	-26.8	329.2
Nemcova	22.9	5.9	125.1
Nevelson	69.8	-35.3	307.8
Ngaio	9.5	-53.3	61.8
Ngone	12.2	6.0	331.9
Nicole	6.4	48.4	259.3
Nightingale	0.0	62.0	132.0
Nijinskaya	36.2	25.8	122.5
Nilanti	9.2	-38.2	331.4
Nilsson	27.3	-75.9	277.6
Nin	27.1	-3.9	266.4
Nina	24.6	-55.5	238.7
Ninzi	7.1	15.9	331.7
Nofret	22.5	-58.8	252.2
Nomeda	10.4	-49.2	55.5
Noreen	18.6	33.6	22.7
Noriko	7.5	-5.3	358.3
Nsele	5.1	6.7	64.2
Nuon	6.5	78.6	336.6
Nuriet	17.9	20.6	245.6
Nutsa	8.0	27.5	341.2
Nyal ga	5.5	17.0	64.5
Nyele	11.9	-22.7	318.4
Nyogari	13.0	-46.4	306.4
Oakley	18.4	-29.3	310.5
Obukhova	46.0	70.7	289.7
O Connor	30.4	-26.0	143.9
Odarka	7.0	40.8	138.2
Odikha	10.6	-41.6	238.1
Odilia	20.8	81.2	200.2
Ogulbek	6.5	2.4	145.0
Oivit	4.8	-73.9	195.5
O Keeffe	76.9	24.5	228.8
Oksana	7.7	11.9	352.0
Oku	13.3	-64.2	232.2
Olena	7.0	10.9	149.0
Olesnicka	33.0	18.3	210.9
Olesya	12.0	5.6	273.3
Olga	15.5	26.1	283.8
Olivia	10.2	37.2	207.9
Olya	13.4	51.4	291.8
Oma	7.6	-42.7	329.1
Onissya	8.2	-25.6	150.2
Opika	9.8	-57.1	151.9
Orczy	26.9	3.7	52.3

continued ...

Table A.1: All Venusian Impact Craters after (Herrick and Phillips, 1994b) - continued .

Feature Name	Diameter	Latitude	Longitude
Orguk	11.7	-23.5	198.2
Orlette	12.5	-68.1	193.3
Orlova	19.6	56.5	235.0
Ortensia	7.0	7.6	155.7
Oshalche	8.3	29.7	155.5
Osipenko	30.0	71.2	321.0
Ottavia	12.9	-47.5	187.1
Outi	10.5	61.6	267.7
Paige	6.8	-1.2	24.6
Pamela	14.2	11.0	238.5
Parishan	6.8	-0.2	146.5
Parra	42.4	20.5	78.5
Parvina	7.0	-62.2	153.0
Pasha	7.2	42.7	156.3
Pat	10.1	2.9	262.6
Patimat	5.1	-1.3	156.5
Patti	47.0	35.0	301.6
Pavlinka	7.5	-25.5	158.7
Pavlova	38.0	14.6	39.2
Peck	30.4	-28.9	294.3
Peggy	11.9	-20.4	357.2
Pena	29.6	-23.6	190.6
Phaedra	15.7	35.9	252.7
Philomena	14.8	-40.7	151.9
Phryne	39.4	-46.2	314.7
Phyllis	11.4	12.3	132.4
Piaf	39.1	0.8	5.3
Piret	27.0	37.8	41.7
Pirkko	12.3	44.8	254.6
Piscopia	26.2	1.5	190.9
Polenova	41.0	-45.5	335.5
Polina	21.6	42.4	148.2
Ponselle	57.7	-63.0	289.1
Potanina	94.2	31.6	53.1
Potter	46.9	7.2	309.1
Prichard	23.3	44.0	11.5
Puhioia	5.5	20.6	69.4
Purev	11.6	-31.1	46.4
Pychik	10.1	-62.4	33.8
Qarlygha	9.3	-33.0	162.9
Quimby	23.2	-5.7	76.7
Qulzhan	7.9	23.5	165.4
Quslu	8.7	6.2	166.8
Rachel	12.5	-48.7	13.5
Radhika	7.9	-30.3	166.4
Radka	10.5	75.6	96.3
Radmila	5.2	69.1	167.0
Rae	5.5	-8.9	58.4
Rafiga	5.7	62.9	175.6
Raisa	13.5	27.5	280.3
Raki	7.5	-49.4	70.0
Rampyari	7.7	50.6	179.3
Rand	24.3	-63.8	59.5
Rani	10.7	64.1	160.4
Raymonde	5.3	48.4	191.5
Rebecca	9.5	-12.1	5.4

continued ...

Table A.1: All Venusian Impact Craters after (Herrick and Phillips, 1994b) - continued .

Feature Name	Diameter	Latitude	Longitude
Recamier	25.3	-12.6	58.1
Regina	24.9	30.0	147.3
Reiko	9.7	22.6	192.1
Retno	7.2	-52.9	192.3
Rhoda	12.2	11.4	347.7
Rhys	44.0	8.6	298.8
Richards	25.0	2.5	196.1
Riley	20.2	14.1	72.5
Rita	8.3	71.0	334.8
Romanskaya	30.4	23.2	178.4
Romola	17.5	9.3	54.2
Roptyna	11.5	62.2	28.9
Rosa Bonheur	104.0	9.7	288.8
Rose	15.5	-35.2	248.2
Rossetti	23.4	57.0	6.4
Rowena	19.5	10.4	171.4
Roxanna	9.5	26.5	334.6
Royle	6.1	-32.7	193.7
Rudneva	29.8	78.4	174.7
Rufina	5.0	-74.6	195.1
Ruit	6.4	-25.5	72.9
Runak	7.6	-58.5	196.3
Ruslanova	44.3	83.9	16.6
Ruth	18.5	43.3	19.9
Sabin	33.1	-38.5	274.7
Sabira	15.7	-5.8	239.9
Safarmo	7.4	-10.8	161.4
Saida	9.5	28.2	302.0
Salika	12.5	-5.0	97.7
Samantha	16.9	45.6	281.7
Samintang	25.9	-39.0	80.7
Sandel	17.9	-45.7	211.7
Sandi	12.6	-68.1	315.1
Sandugach	10.0	59.9	143.5
Sanger	83.6	33.8	288.6
Sanija	18.0	33.1	251.0
Saodat	3.7	-2.9	344.6
Sarah	18.5	-42.4	1.8
Sartika	18.7	-63.4	67.0
Sasha	4.6	38.3	277.3
Saskia	37.1	-28.6	337.1
Sayers	98.0	-67.5	229.8
Sayligul	4.3	73.6	172.9
Scarpellini	27.1	-23.2	34.6
Seiko	3.4	-21.0	216.6
Selma	11.4	68.5	155.9
Seseg	9.8	-36.3	312.6
Sevigne	29.6	52.6	326.5
Seymour	63.0	18.2	326.5
Shakira	17.6	3.0	213.6
Shasenem	9.0	-44.0	258.9
Sheila	5.6	19.9	50.2
Shih Mai Yu	22.3	18.4	318.9
Shirley	18.0	31.5	55.4
Shushan	8.5	-43.8	70.2
Siddons	47.0	61.6	340.6

continued ...

Table A.1: All Venusian Impact Craters after (Herrick and Phillips, 1994b) - continued .

Feature Name	Diameter	Latitude	Longitude
Sidney	20.2	13.4	199.6
Sigrid	16.2	63.6	314.4
Simbya	4.0	-74.4	130.0
Simone	14.0	59.5	82.0
Simonenko	31.9	-26.9	97.6
Sirani	28.3	-31.5	230.4
Sitwell	32.8	16.6	190.4
Solace	5.3	35.9	317.2
Sophia	17.6	-28.6	18.8
Sovadi	12.4	-44.8	225.5
Stanton	107.0	-23.3	199.3
Stefania	11.7	51.3	333.3
Stein	13.3	-30.1	345.5
Steinbach	20.3	-41.4	256.9
Stina	10.4	37.4	22.8
Storni	21.7	-9.8	245.6
Stowe	80.0	-43.2	233.2
Stuart	68.6	-30.8	20.2
Suliko	14.9	9.6	214.6
Sullivan	32.0	-1.4	110.9
Surija	15.3	5.3	178.2
Susanna	13.3	6.0	93.3
Sveta	21.0	82.5	273.2
Taglioni	31.0	41.7	122.6
Tahia	6.1	44.3	73.7
Taira	19.6	-1.6	296.8
Tako	10.7	25.1	285.3
Talvikki	12.6	41.9	22.0
Tamara	11.0	61.6	317.2
Tanya	14.0	-19.3	282.7
Tatyana	19.0	85.4	212.4
Taussig	25.8	-9.2	229.0
Tehina	5.4	-30.4	76.4
Tekarohi	9.3	21.2	76.4
Temou	9.3	-10.0	83.4
Teresa	14.8	-42.5	10.0
Terhi	10.7	45.7	253.1
Teroro	9.2	-75.8	88.1
Teumere	5.4	-38.3	88.1
Teura	9.3	-12.3	90.2
Thomas	25.2	-13.0	272.5
Tiffany	7.0	-8.7	22.9
Tinyl	12.8	9.7	132.1
Toklas	17.5	0.7	273.1
Tolgonay	4.6	68.8	271.1
Trollope	27.2	-54.8	246.4
Truth	47.3	28.7	287.8
Tseraskaya	30.3	28.6	79.2
Tsetsa	9.9	31.3	317.7
Tsiala	16.5	2.9	100.0
Tsvetayeva	42.9	64.6	147.4
Tsyrma	7.8	-14.1	318.5
Tubman	42.9	23.6	204.6
Tunde	16.3	76.8	193.0
Tursunoy	4.7	80.9	229.3
Tussaud	16.0	21.7	221.0

continued ...

Table A.1: All Venusian Impact Craters after (Herrick and Phillips, 1994b) - continued .

Feature Name	Diameter	Latitude	Longitude
Tuyara	13.2	-62.9	15.5
Ualinka	8.1	13.2	168.6
Udagan	11.5	10.7	206.9
Udaltsova	26.7	-20.3	275.3
Udyaka	7.7	30.9	172.9
Ugne	10.3	34.9	205.8
Uleken	10.9	33.7	185.1
Ulla	10.4	-51.5	184.5
Ulpu	7.0	-35.7	179.0
Ulrique	19.6	75.9	55.6
Uluk	10.3	-62.2	178.6
Ul yana	12.5	24.3	253.0
Umaima	6.9	-23.3	195.4
Umkana	6.2	-53.3	198.6
Unay	11.4	53.5	172.7
Undset	20.0	51.7	60.8
Unitkak	8.0	40.8	199.5
Urazbike	7.0	-9.0	202.5
Ustinya	11.8	-41.2	251.6
Uvaysi	38.9	2.3	198.3
Uyengimi	8.9	-76.9	204.9
Vacarescu	31.5	-63.0	199.8
Vaka	11.8	-41.4	8.9
Valadon	25.2	-49.0	167.7
Valborg	20.0	75.5	272.1
Valentina	24.6	46.4	144.1
Valerie	13.6	-6.4	30.9
Vallija	15.2	26.3	120.0
Vanessa	10.0	-6.0	1.9
Vard	6.1	17.5	314.5
Varya	14.3	2.8	211.8
Vashti	17.0	-6.8	43.7
Vasilutsa	5.7	16.5	334.4
Vassi	8.5	34.4	346.5
Veriko	5.2	20.4	350.1
Veronica	17.9	-38.1	124.6
Vesna	14.9	-60.3	220.5
Veta	6.4	42.6	349.5
Vigee Lebrun	57.8	17.3	141.4
Viola	10.0	-36.1	240.5
Virga	10.3	-26.9	7.7
Virginia	18.5	-52.9	185.9
Virve	18.0	-5.1	346.9
Vlasta	10.7	28.4	250.1
Volkova	47.5	75.2	242.2
Volyana	5.3	60.6	359.9
von Paradis	37.5	-32.2	314.9
von Schuurman	29.1	-5.0	191.0
Von Siebold	32.4	-52.0	36.6
von Suttner	24.0	-10.6	234.9
Voynich	48.7	35.4	56.1
Wanda	21.7	71.3	323.1
Wang Zhenyi	23.4	13.2	217.8
Warren	50.9	-11.7	176.5
Wazata	13.9	33.6	298.3
Weil	24.2	19.4	283.1

continued ...

Table A.1: All Venusian Impact Craters after (Herrick and Phillips, 1994b) - continued .

Feature Name	Diameter	Latitude	Longitude
Wendla	5.7	22.5	207.6
Wen Shu	31.5	-5.0	303.7
West	28.8	26.1	303.0
Wharton	50.5	55.7	61.9
Wheatley	74.8	16.6	268.0
Whiting	35.7	-6.1	128.0
Whitney	42.5	-30.2	151.3
Wieck	20.2	-74.2	244.8
Wilder	35.1	17.4	122.6
Willard	48.4	-24.6	296.1
Wilma	12.5	36.7	1.7
Winema	21.7	3.0	168.6
Winnemucca	30.3	-15.4	121.1
Wiwi yokpa	4.5	-73.8	228.4
Wollstonecraft	44.1	-39.1	260.8
Woolf	24.5	-37.7	27.2
Workman	17.4	-12.9	299.9
Wu Hou	27.5	-25.5	317.4
Wynne	10.0	55.0	53.6
Xantippe	40.4	-10.9	11.8
Xenia	13.5	-30.3	249.4
Xiao Hong	38.7	-43.5	101.7
Ximena	12.8	-68.2	243.6
Xi Wang	7.7	14.0	208.0
Yablochkina	64.3	48.3	195.3
Yakyt	13.8	2.1	170.2
Yale	18.5	-13.4	271.2
Yambika	6.5	32.6	208.7
Yasuko	10.6	-26.1	169.0
Yazruk	10.5	21.2	160.2
Yelya	8.6	-47.5	211.7
Yemysh	6.0	11.9	214.7
Yenlik	8.6	-16.0	225.4
Yerguk	6.3	42.7	226.8
Yeska	9.1	27.4	230.1
Yetta	9.0	58.6	185.4
Yokhtik	11.4	-50.1	158.1
Yoko	5.0	-5.7	232.0
Yolanda	11.4	7.8	152.7
Yomile	13.6	-27.3	138.7
Yonge	42.8	-14.0	115.1
Yonok	9.5	-65.1	234.1
Yonsuk	8.5	-34.0	234.8
Yoshioka	16.6	-32.4	59.0
Ytunde	6.1	49.9	81.1
Yvette	10.6	7.5	249.6
Yvonne	14.5	-56.0	298.4
Zakiya	7.5	-66.5	234.1
Zamudio	19.0	9.6	189.3
Zarema	5.0	16.8	235.2
Zdravka	12.5	65.1	299.0
Zeinab	12.5	-2.2	159.6
Zemfira	11.4	-46.2	157.7
Zenobia	39.1	-29.3	28.6
Zerine	6.5	-29.6	258.6
Zhilova	53.0	66.3	125.7

continued ...

Table A.1: All Venusian Impact Craters after (Herrick and Phillips, 1994b) - continued .

Feature Name	Diameter	Latitude	Longitude
Zhu Shuzhen	29.4	-26.5	356.5
Zija	16.8	-3.5	265.0
Zina	9.0	41.9	320.1
Zivile	13.5	48.8	113.1
Zlata	7.0	64.6	333.9
Zosia	10.5	-18.9	109.2
Zoya	20.0	69.1	236.2
Zuhrah	5.8	34.7	357.0
Zula	5.0	7.3	282.0
Zulfiya	12.9	18.4	101.9
Zulma	11.0	-7.7	102.0
Zumrad	12.9	32.1	94.8
Zurka	5.5	-12.8	275.2
Zvereva	22.9	45.4	283.1

A.2 Table of all Venusian Polygonal Impact Craters

Table A.2: All Venusian Polygonal Impact Craters (PICs), after (Öhman, 2009).

Feature Name	Diameter	Latitude	Longitude
Abigail	18.5	-52.2	111.2
Agnesi	41.4	-39.5	37.7
Agrippina	38.4	-33.3	65.7
Aimee	16.8	16.1	127.2
Aita	14.1	8.9	270.7
Andreianova	69.5	-3.0	68.7
Anush	12.2	14.9	86.5
Anya	17.7	39.5	297.8
Austen	43.9	-25.0	168.5
Ayana	14.9	-29.2	175.5
Ban Zhao	38.3	17.2	146.9
Behn	25.8	-32.5	142.0
Bineta	12.4	57.2	144.1
Blixen	21.0	-60.2	145.7
Bly	22.4	37.7	305.6
Bradstreet	35.2	16.5	47.7
Brooke	22.5	48.4	296.6
Bugoslavskaya	29.7	-23.0	300.4
Carson	37.6	-24.2	344.1
Castro	22.6	3.3	233.9
Colleen	14.0	-60.8	162.2
Comnena	19.0	1.2	343.7
Corinna	18.5	22.9	40.6
Cynthia	15.8	-16.7	347.5
Datsolalee	17.0	38.3	171.8
de Beauvoir	53.3	2.0	96.1
de Lalande	21.6	20.4	355.0
de Stael	22.8	37.4	324.2
De Witt	20.7	-6.5	275.6
Devorguilla	23.1	15.3	4.0
Dolores	12.5	51.4	201.6
Durant	21.1	-62.3	227.6
Elza	16.9	-34.4	275.9
Erin	13.9	-47.0	184.8
Evangeline	15.9	69.6	222.0
Evika	19.8	-5.1	31.4
Fatima	14.7	-17.8	31.9
Frank	22.6	-13.1	12.9
Fredegonde	24.9	-50.5	93.3
Galindo	24.0	-23.3	258.9
Gina	14.5	78.1	76.5
Gretchen	21.2	-59.7	213.2
Grimke	34.6	17.3	215.3
Guilbert	26.1	-58.0	13.6
Halle	21.1	-19.8	145.5
Hannah	19.1	17.9	102.6
Henie	68.7	-52.0	146.0
Horner	24.7	23.4	97.8
Howe	38.5	-45.7	174.8
Huang Daopo	27.2	-54.2	165.3
Hwangcini	30.8	6.3	141.7
Inira	17.0	-43.1	239.4
Irene	13.5	49.8	134.0

continued ...

Table A.2: All Venusian Polygonal Impact Craters (PICs), after (Öhman, 2009) - continued

Feature Name	Diameter	Latitude	Longitude
Jocelyn	13.5	-33.3	276.4
Johnson	24.0	51.8	254.6
Juanita	19.4	-62.8	90.0
Kaikilani	19.6	-32.8	163.2
Kastusha	12.7	-28.6	60.0
Ketzia	14.5	4.0	300.5
Laulani	12.3	-68.2	121.2
Laura	18.4	48.9	141.2
Lehmann	22.8	-44.1	39.1
Leila	19.3	-44.2	86.8
Lydia	15.0	10.7	340.7
Margit	13.6	60.0	273.1
Marie	14.5	-21.7	232.4
Marsh	47.4	-63.6	46.6
Mead	268.7	12.5	57.0
Megan	15.6	-61.8	130.6
Merian	21.9	34.5	76.2
Monika	26.1	72.3	122.4
Moses	28.1	34.6	119.9
Mowatt	36.7	-14.6	292.3
Mu Guiying	32.7	41.2	81.1
Muriel	18.8	-41.7	12.4
Nadine	18.8	7.8	359.1
Ngone	12.6	6.0	331.9
Nofret	22.9	-58.8	252.1
Nyogari	12.2	-46.5	306.4
Oakley	17.5	-29.3	310.5
Odilia	20.4	81.3	200.4
Pamela	13.9	11.0	238.5
Phryne	37.6	-46.1	314.7
Piscopia	24.8	1.5	190.9
Quimby	22.9	-5.7	76.7
Rand	25.2	-63.8	59.5
Rhys	44.0	8.6	298.8
Romola	19.1	9.3	54.2
Sabira	16.0	-5.8	239.8
Sarah	19.5	-42.4	1.8
Sayers	93.6	-67.5	229.6
Scarpellini	27.2	-23.3	34.6
Shakira	18.5	3.0	213.6
Sirani	27.7	-31.5	230.4
Susanna	13.2	6.0	93.3
Tanya	14.2	-19.3	282.8
Thomas	25.9	-13.0	272.5
Toklas	17.2	0.7	273.1
Tsiala	16.0	2.9	100.0
Tuyara	12.2	-62.9	15.5
Uvaysi	38.0	2.3	198.2
Vacarescu	30.6	-63.0	199.8
Valentina	24.3	46.4	144.1
Valerie	13.9	-6.4	30.9
Vashti	16.5	-6.8	43.7
Veronica	17.9	-38.1	124.6
Vigee-Lebrun	57.6	17.3	141.4
Virginia	18.1	-52.9	185.9
von Schuurman	28.9	-5.0	191.0

continued ...

Table A.2: All Venusian Polygonal Impact Craters (PICs), after (Öhman, 2009) - continued

Feature Name	Diameter	Latitude	Longitude
Wanda	19.8	71.2	323.1
Wazata	14.0	33.6	298.3
Weil	23.4	19.3	283.1
West	28.0	26.1	303.0
Wilma	13.0	36.7	1.7
Woolf	24.6	-37.7	27.2
Yoshioka	16.7	-32.4	58.9
Yvonne	15.2	-56.0	298.4
Zdravka	12.0	65.1	299.1
Zija	18.2	-3.5	265.0
Zulfiya	12.3	18.4	101.9
Zvereva	22.3	45.3	283.1

A.3 Images of the selected and screened PICs

The images of all 22 selected and screened polygonal impact craters including data for position (latitude, longitude) and diameter

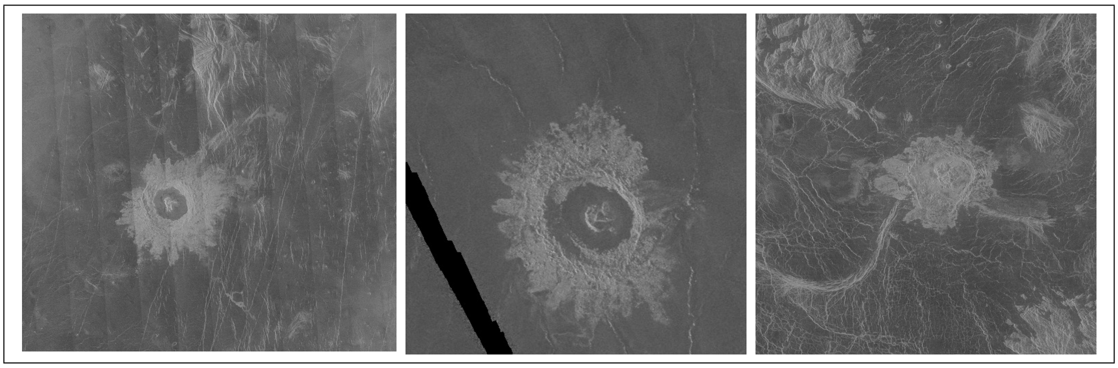

Figure A.1: Crater Hwangcini 6.3N 141.7E 30.2 km, Crater Vacarescu 63.0S 199.8E 31.5 km, Crater Mu Guiying 41.2N 81.1E 32.3 km (IAU/USGS/NASA-Planetary-Database, 2013).

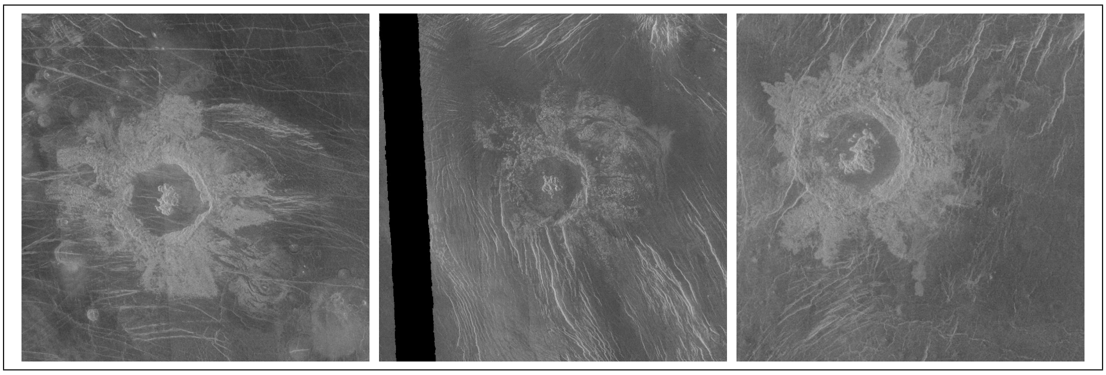

Figure A.2: Crater Grimke 17.3N 215.3E 34.8 km, crater Bradstreet 16.5N 047.7E 36.0 km, Crater Mowatt 14.6S 292.3E 36.7 km (IAU/USGS/NASA-Planetary-Database, 2013).

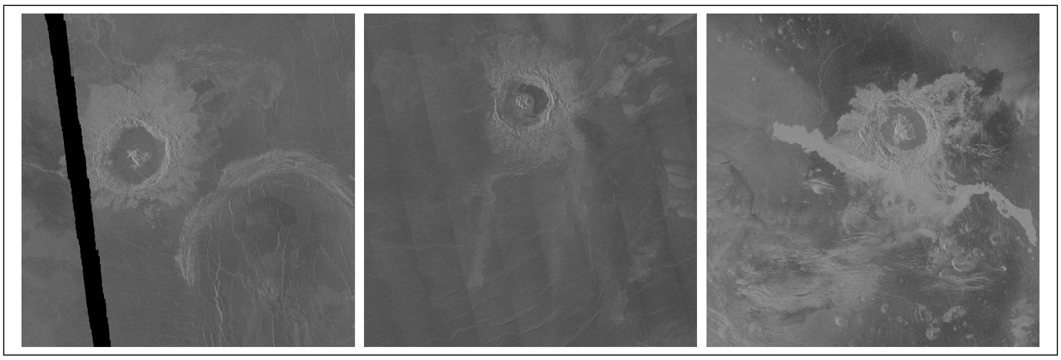

Figure A.3: Crater Agrippina 33.3S 065.7E 38.4 km, Crater Howe 45.7S 174.8E 36.6 km, Crater Carson 24.2S 344.1E 38.8 km (IAU/USGS/NASA-Planetary-Database, 2013).

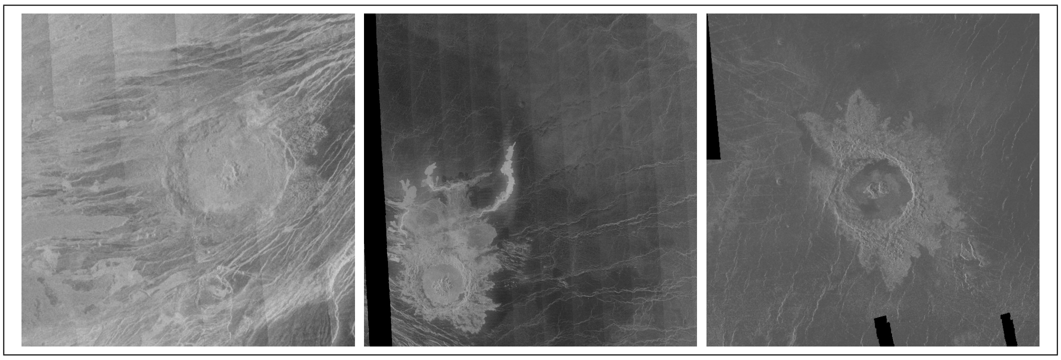

Figure A.4: Crater Uvaysi 02.3N 198.2E 38.9 km, Crater Ban Zhao 17.2N 146.9E 39.0 km, Crater Phryne 46.1S 314.7E 42.4 km (IAU/USGS/NASA-Planetary-Database, 2013).

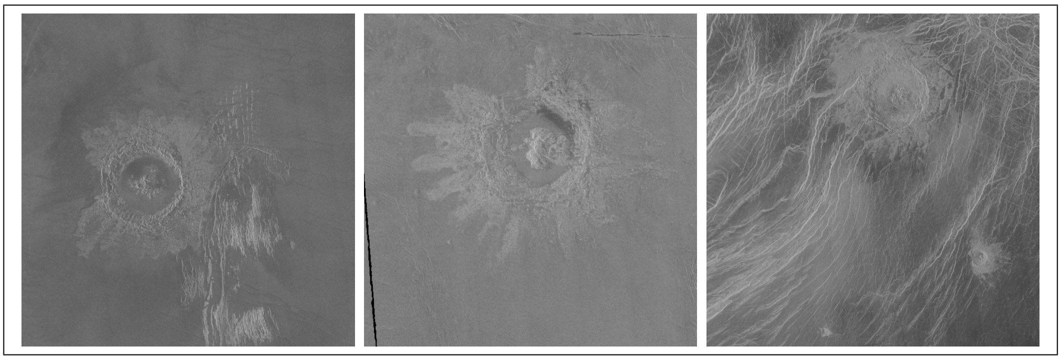

Figure A.5: Crater Agensi 39.5S 037.7E 42.4 km, Crater Rhys 08.6N 298.8E 44.0 km, Crater Austen 25.0S 168.5E 45.1 km (IAU/USGS/NASA-Planetary-Database, 2013).

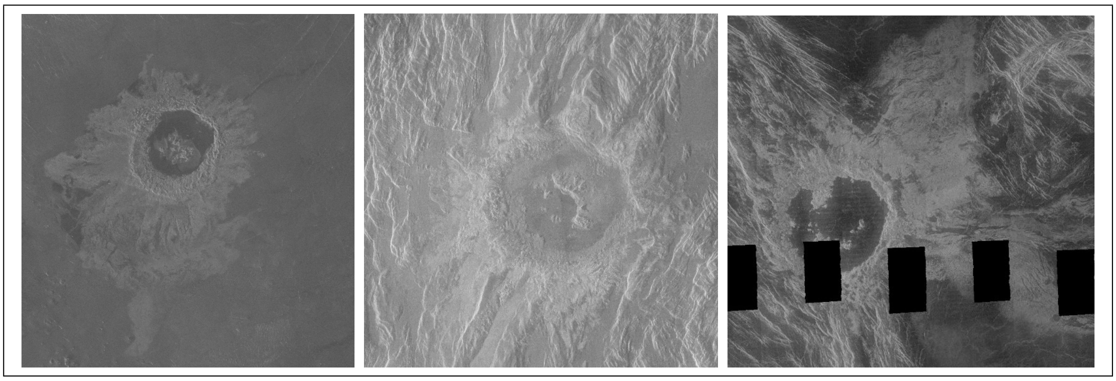

Figure A.6: Crater Marsh 63.6S 046.6E 47.7 km, Crater de Beauvoir 02.0N 096.1E 52.5 km, Crater Vigee Lebrun 17.3N 141.4E 57.8 km (IAU/USGS/NASA-Planetary-Database, 2013).

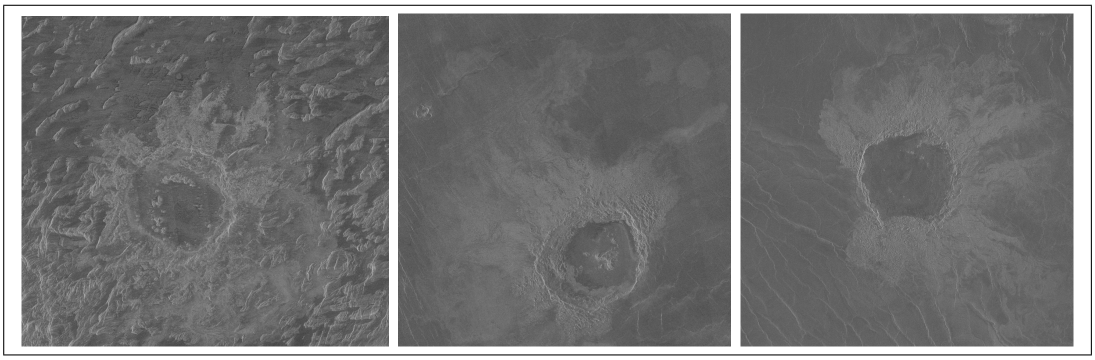

Figure A.7: Crater Andreianova 03.0 S 068.7E 66.1 km, Crater Henie 52.0S 146.0E 70.4km, Crater Sayers 67.5S 229.6E 98.0 km (IAU/USGS/NASA-Planetary-Database, 2013).

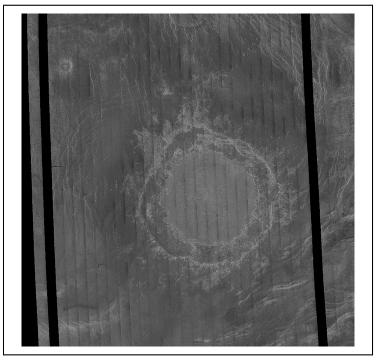

Figure A.8: Crater Mead 12.5N 057.0E 270.0 km (IAU/USGS/NASA-Planetary-Database, 2013).

References

Aittola, M., Öhman, T., Leitner, J. J., Kostama, V.-P., and Raitala, J. (2010). The structural control of venusian polygonal impact craters. Icarus, 205:356–363.

Aittola, M., Öhman, T., Leitner, J. J., and Raitala, J. (2007). The Characteristics of Polygonal Impact Craters on Venus. *Earth Moon and Planets*, 101:41–53.

Baker, V. R., Komatsu, G., Gulick, V. C., and Parker, T. J. (1997). Channels and Valleys. In Bougher, S. W., Hunten, D. M., and Phillips, R. J., editors, *Venus II: Geology, Geophysics, Atmosphere, and Solar Wind Environment*, page 757.

Barsukov, V. L., Basilevsky, A. T., Burba, G. A., Bobinna, N. N., Kryuchkov, V. P., Kuzmin, R. O., Nikolaeva, O. V., Pronin, A. A., Ronca, L. B., Chernaya, I. M., Shashkina, V. P., Garanin, A. V., Krushky, E. R., Markov, M. S., Sukhanov, A. L., Kotelnikov, V. A., Rzhiga, O. N., Petrov, G. M., Alexandrov, Y. N., Sidorenko, A. I., Bogomolov, A. F., Skrypnik, G. I., Bergman, M. Y., Kudrin, L. V., Bokshtein, I. M., Kronrod, M. A., Chochia, P. A., Tyuflin, Y. S., Kadnichansky, S. A., and Akim, E. L. (1986). The geology and geomorphology of the Venus surface as revealed by the radar images obtained by Veneras 15 and 16. J. Geophys. Res., 91:378–D398.

Basilevsky, A. T. and Head, J. W. (2000). Rifts and large volcanoes of Venus: Global assessment of their age relations with regional plains. J. Geophys. Res., 105:24583–24612.

Basilevsky, A. T. and Head, J. W. (2002a). Venus: Analysis of the degree of impact crater deposit degradation and assessment of its use for dating geological units and features. J. Geophys. Res.*Planet*, 107:5061.

Basilevsky, A. T. and Head, J. W. (2003). The surface of Venus. *Reports on Progress in Physics*, 66:1699–1734.

Basilevsky, A. T. and Head, J. W. (2006). Impact craters on regional plains on Venus: Age relations with wrinkle ridges and implications for the geological evolution of Venus. J. Geophys. Res.*Planet*, 111(E10):3006.

Basilevsky, A. T., Head, J. W., and Setyaeva, I. V. (2003). Venus: Estimation of age of impact craters on the basis of degree of preservation of associated radar-dark deposits. *grl*, 30:1950.

Basilevsky, A. T. and Head, III, J. W. (2002b). Venus: Dating Post-Regional-Plains Formations Through Analysis of Preservation of Crater-associated Radar-Dark Deposits. In *Lunar and Planetary Institute Science Conference Abstracts*, volume 33 of *Lunar and Planetary Institute Science Conference Abstracts*, page 1006.

Bilotti, F. and Suppe, J. (1999). The Global Distribution of Wrinkle Ridges on Venus. Icarus, 139:137–157.

Cochrane, C. G. and Ghail, R. C. (2006). Topographic constraints on impact crater morphology on Venus from high-resolution stereo synthetic aperture radar digital elevation models. J. Geophys. Res.*Planet*, 111:4007.

Croft, S. K. (1985). The scaling of complex craters. In Ryder, G. and Schubert, G., editors, *Lunar and Planetary Science Conference Proceedings*, volume 15 of *Lunar and Planetary Science Conference Proceedings*, page 828.

Eppler, D. T., Ehrlich, R., Nummedal, D., and Schultz, P. H. (1983). Sources of Shape Variation in Lunar Impact Craters – Fourier Shape Analysis. In *Lunar and Planetary Institute Science Conference Abstracts*, volume 13 of *Lunar and Planetary Institute Science Conference Abstracts*, pages 203–204.

French, B. M. (1998). *Traces of Catastrophe: A Handbook of Shock-Metamorphic Effects in Terrestrial Meteorite Impact Structures.* Lunar and Planetary Institute, Houston. 120 pp.

Guseva, E. N., Basilevsky, A. T., and Head, J. W. (2013). Estimation of the age of impact craters and other adjacent geological subdivisions within the Thetis Regio on Venus. *Solar System Research*, 47:159–169.

Hansen, V. L. and Willis, J. J. (1997). Ribbon terrain formation and implications for lithosphere evolution, Venus. In *Lunar and Planetary Science Conference*, volume 28 of *Lunar and Planetary Science Conference*, page 507.

Hartmann, W. K. and Neukum, G. (2001). Cratering Chronology and the Evolution of Mars. *ssr*, 96:165–194.

Herrick, R. R. and Phillips, R. J. (1994a). Effects of the Venusian atmosphere on incoming meteoroids and the impact crater population. Icarus, 112:253–281.

Herrick, R. R. and Phillips, R. J. (1994b). Implications of a global survey of venusian impact craters. Icarus, 111:387–416.

Herrick, R. R., Sharpton, V. L., Malin, M. C., Lyons, S. N., and Feely, K. (1997). Morphology and Morphometry of Impact Craters. In Bougher, S. W., Hunten, D. M., and Phillips, R. J., editors, *Venus II: Geology, Geophysics, Atmosphere, and Solar Wind Environment*, page 1015.

Huppert, H. E. and Brian Dade, W. (1998). Natural Disasters: Explosive Volcanic Eruptions and Gigantic Landslides. *Theoretical and Computational Fluid Dynamics*, 10:201–212.

IAU/USGS/NASA-Planetary-Database (2013). Gazetteer of Planetary Nomenclature, International Astronomical Union (IAU) Working Group for Planetary System Nomenclature (WGPSN) , http://planetarynames.wr.usgs.gov/.

Ivanov, M. A. and Basilevsky, A. T. (1993). Density of impact craters on tessera, Venus. In *Lunar and Planetary Institute Science Conference Abstracts*, volume 24 of *Lunar and Planetary Inst. Technical Report*, pages 693–694.

Ivanov, M. A. and Head, J. W. (1996). Tessera terrain on Venus: A survey of the global distribution, characteristics, and relation to surrounding units from Magellan data. J. Geophys. Res., 101:14861–14908.

Ivanov, M. A. and Head, J. W. (2001). Geology of Venus: Mapping of a global geotraverse at 30 N latitude. J. Geophys. Res., 106:17515–17566.

Ivanov, M. A. and Head, J. W. (2011). Global geological map of Venus. *planss*, 59:1559–1600.

Izenberg, N. R. and Arvidson, R. E. (1994). Relationships Among Radar Backscatter, Microwave Emissivity, Altitude, and Geology in Ovda Regio, Venus. In *Lunar and Planetary Institute Science Conference Abstracts*, volume 25 of *Lunar and Planetary Inst. Technical Report*, page 605.

Le Feuvre, M. and Wieczorek, M. A. (2011). Nonuniform cratering of the Moon and a revised crater chronology of the inner Solar System. Icarus, 214:1–20.

McGill, G. E. (1993). Wrinkle ridges, stress domains, and kinematics of venusian plains. Geophys. Res. Lett., 20:2407–2410.

McGill, G. E. (2004). Tectonic and stratigraphic implications of the relative ages of venusian plains and wrinkle ridges. Icarus, 172:603–612.

McKinnon, W. B., Zahnle, K. J., Ivanov, B. A., and Melosh, H. J. (1997). Cratering on Venus: Models and Observations. In Bougher, S. W., Hunten, D. M., and Phillips, R. J., editors, *Venus II: Geology, Geophysics, Atmosphere, and Solar Wind Environment*, page 969.

Melosh, H. J. (1989). *Impact cratering: A geologic process.* New York, Oxford University Press (Oxford Monographs on Geology and Geophysics, No. 11), 1989, 253 p.

Melosh, H. J. and Gaffney, E. S. (1983). Acoustic fluidization and the scale dependence of impact crater morphology. J. Geophys. Res., 88:830–834.

Melosh, H. J. and Ivanov, B. A. (1999). Impact Crater Collapse. *Annual Review of Earth and Planetary Sciences*, 27:385–415.

Michael, G. G. and Neukum, G. (2010). Planetary surface dating from crater size-frequency distribution measurements: Partial resurfacing events and statistical age uncertainty. *Earth and Planetary Science Letters*, 294:223–229.

Namiki, N. and Solomon, S. C. (1994). Impact Crater Densities on Volcanoes and Coronae on Venus: Implications for Volcanic Resurfacing. *Science*, 265:929–933.

NASA-Planetary-Fact-Sheet (2013). NASA Planetary Fact Sheet, http://nssdc.gsfc.nasa.gov/planetary/factsheet/ (called 10.10.2013).

Neukum, G. and Ivanov, B. (1994). The Inner Solar System Impact Record: Lunar, Terrestrial-Planet, and Asteroid Size-Frequency Data Comparison. In *Lunar and Planetary Institute Science Conference Abstracts*, volume 25 of *Lunar and Planetary Inst. Technical Report*, page 991.

Neukum, G. and Ivanov, B. A. (2001). Crater Production Function for Mars. In *Lunar and Planetary Institute Science Conference Abstracts*, volume 32 of *Lunar and Planetary Institute Science Conference Abstracts*, page 1757.

Öhman, T. (2009). *The structural control of polygonal impact craters.* PhD thesis, University of Oulu.

Öhman, T., Aittola, M., Kostama, V.-P., Hyvärinen, M., and Raitala, J. (2006). Polygonal impact craters in the Argyre region, Mars: Evidence for influence of target structure on the final crater morphology. *Meteoritics and Planetary Science*, 41:1163–1173.

Öhman, T., Aittola, M., Kostama, V.-P., and Raitala, J. (2005). The Preliminary Analysis of Polygonal Impact Craters within Greater Hellas Region, Mars. In C. Koeberl & H. Henkel, editor, *Impact Tectonics*, page 131.

Phillips, R. J., Arvidson, R. E., Boyce, J. M., Campbell, D. B., Guest, J. E., Schaber, G. G., and Soderblom, L. A. (1991). Impact craters on Venus - Initial analysis from Magellan. *Science*, 252:288–297.

Phillips, R. J., Raubertas, R. F., Arvidson, R. E., Sarkar, I. C., Herrick, R. R., Izenberg, N., and Grimm, R. E. (1992). Impact craters and Venus resurfacing history. J. Geophys. Res., 97:15923.

Pike, R. J. (1976). Simple to Complex Impact Craters: The Transition on the Moon. In *Lunar and Planetary Science Conference*, volume 7 of *Lunar and Planetary Science Conference*, page 700.

Poelchau, M. H., Kenkmann, T., and Kring, D. A. (2009). Rim uplift and crater shape in Meteor Crater: Effects of target heterogeneities and trajectory obliquity. J. Geophys. Res.*Planet*, 114(13):E01006.

Price, M. and Suppe, J. (1994). Mean age of rifting and volcanism on Venus deduced from impact crater densities. Nature, 372:756–759.

Roddy, D. J. (1977). Large-scale impact and explosion craters - Comparisons of morphological and structural analogs. In Roddy, D. J., Pepin, R. O., and Merrill, R. B., editors, *Impact and Explosion Cratering: Planetary and Terrestrial Implications*, pages 185–246.

Schaber, G. G. (1982). Venus - Limited extension and volcanism along zones of lithospheric weakness. Geophys. Res. Lett., 9:499–502.

Schaber, G. G., Strom, R. G., Moore, H. J., Soderblom, L. A., Kirk, R. L., Chadwick, D. J., Dawson, D. D., Gaddis, L. R., Boyce, J. M., and Russell, J. (1992). Geology and distribution of impact craters on Venus: What are they telling us? J. Geophys. Res.*Planet*, 97(E16):13257.

Schenk, P. and Sharpton, V. L. (1992). The Simple-to-Complex Crater Transition on Venus. In *Lunar and Planetary Institute Science Conference Abstracts*, volume 23 of *Lunar and Planetary Institute Science Conference Abstracts*, page 1219.

Stofan, E. R., Hamilton, V. E., Janes, D. M., and Smrekar, S. E. (1997). Coronae on Venus: Morphology and Origin. In Bougher, S. W., Hunten, D. M., and Phillips, R. J., editors, *Venus II: Geology, Geophysics, Atmosphere, and Solar Wind Environment*, page 931.

Strom, R. G., Schaber, G. G., Arkani-Hamed, J., and Toksoz, M. N. (1992). Global Resurfacing of Venus. In *Lunar and Planetary Institute Science Conference Abstracts*, volume 23 of *Lunar and Planetary Inst. Technical Report*, page 1379.

Strom, R. G., Schaber, G. G., and Dawsow, D. D. (1994). The global resurfacing of Venus. J. Geophys. Res., 99:10899.

Surkov, I. A. (1982). The natural radioactivity of rocks of the moon and planets. *Geokhimiia*, pages 755–766.

Turcotte, D. L. (1993). An episodic hypothesis for venusian tectonics. J. Geophys. Res., 98:17061–17068.

Turcotte, D. L. (1997). How does the interior of Venus lose heat? In *Lunar and Planetary Institute Science Conference Abstracts*, volume 28 of *Lunar and Planetary Institute Science Conference Abstracts*, page 1457.

Turcotte, D. L., Morein, G., Roberts, D., and Malamud, B. D. (1999). Catastrophic Resurfacing and Episodic Subduction on Venus. Icarus, 139:49–54.

Watters, T. R. (1988). Wrinkle ridge assemblages on the terrestrial planets. J. Geophys. Res., 93:10236–10254.

Weihs, G. T., Leitner, J. J., and Firneis, M. G. (2012). Polygonal Impact Craters on Mercury. In *Lunar and Planetary Institute Science Conference Abstracts*, volume 43 of *Lunar and Planetary Inst. Technical Report*, page 1083.

Weitz, C. M. and Basilevsky, A. T. (1993). Magellan observations of the Venera and Vega landing site regions. J. Geophys. Res., 98:17069–17098.

Wood, C. A. and Andersson, L. (1978). Lunar Crater Morphometry: New Data. In *Lunar and Planetary Institute Science Conference Abstracts*, volume 9 of *Lunar and Planetary Institute Science Conference Abstracts*, pages 1267–1269.

Zahnle, K. J. and McKinnon, W. B. (1997). The Age of the Surface of Venus. *NASA STI/Recon Technical Report N*, 2:47559.

List of Figures

List of Tables

Abstract

A Polygonal Impact Crater (PIC) is an impact crater, the shape of which in plan view is not circular but more or less angular, and its rims are composed of at least two adjacent straight segments (Aittola et al., 2007). Former researches have proven that polygonal impact craters are also found on the Moon, on Mercury, Mars, Venus, and on several asteroids and icy moons. On Venus there exists no large population of polygonal impact craters, and therefore there is no statistically reliable base to analyze their correlation with the local vicinity. Older studies indicated that there exist regions where the orientations of straight rim segments seem to align with tectonic features lying close to the craters and showed that the orientations of the straight rims in many cases reflect the local tectonics and 'zones of weaknesses', which might be useful tools to determine the young surface tectonic structures. From the approximately 900 impact craters on Venus a list of 121 PICs were identified by [4], from which we selected a set of 22 PICs on Venus with a diameter . In this study a set of 22 PICs on Venus with a diameter greater than 30 km was selected from a list of PICs identified by Öhman, 2009 and screened. The age of these PICs, which are completely or partially superposed on regional plains was estimated in relation to the regional plains. This type of volcanic plains dominates the entire surface of Venus and usually is deformed by wrinkle ridges. The findings demonstrated that the mean age of PICs in relation to the surrounding regional plains is evidently younger. The results of the analysis were compared to similar studies and a good agreement was achieved.

Zusammenfassung

Ein polygonaler Einschlagskrater (en. Polygonal Impact Crater (PIC)) ist ein Krater, der in der Draufsicht mehr oder weniger eckig erscheint und dessen Kraterränder sich aus mindestens zwei geraden benachbarten Segmenten zusammengesetzen. Frühere Studien haben bewiesen, dass die polygonalen Einschlagskrater auch auf dem Mond, auf Merkur, Mars, Venus und auf mehreren Asteroiden und Eismonden gefunden werden. Auf der Venus gibt es keine großen Populationen von polygonalen Einschlagskrater und deshalb gibt es keine statistisch verlässliche Basis, um ihre Korrelation mit der lokalen Umgebung zu analysieren. Ältere Untersuchungen ergaben, dass es Regionen gibt, in denen sich die geraden Kratersegmente an tektonischen Merkmale in der Nähe der Krater auszurichten scheinen. Weiters zeigten sie, dass diese Ausrichtung der geraden Kraterränder in vielen Fällen die lokalen Tektonik und Zonen verringerter Dichte ('Schwächezonen') anzeigen und damit nützliche Werkzeuge sein könnten, um die Tektonik der jungen Oberfläche zu bestimmen. In dieser Studie wurden die aus einer veröffentlichten Liste (Öhman, 2009) ausgewählte PICs auf der Venus mit einem Durchmesser $\geq$30 km untersucht und 22 PICs, die vollständig oder teilweise regionale Ebenen überlagern ermittelt. Das Alter dieser PICs relativ zu den regionalen Ebenen wurde geschätzt. Dieser Typ vulkanischer Ebenen dominiert die gesamte Oberfläche der Venus und wird in der Regel durch 'wrinkle ridges' verformt. Die Ergebnisse zeigen, dass das mittlere Alter der PICs relativ zu den umliegenden regionalen Ebenen jünger ist. Die Resultate der vorliegenden Untersuchung wurden mit den Ergebnissen ähnlicher Studien verglichen und eine gute Übereinstimmung erreicht.

CURRICULUM VITAE

Personal Data

Name:	Gerhard Weihs
Born:	July 31, 1946, in Vienna, Austria
Family:	married since 1975, widowed since 2010 3 children
Nationality:	Austrian

Scientific Education

1964	School-leaving examination at Bundesrealschule Wien 7, Neustiftgasse
1964	Study of Technical Physics, Technical University of Vienna, Austria
1974	Diploma in Physics, Institute of Applied Physics, TU Vienna Diploma thesis, 'Untersuchungen im Dreistoffsystem Y - Fe - Ni', supervisor: Univ.Prof. Dr. F. Lihl
2009	Study of Astronomy , University of Vienna, Austria
2012	Bachelor of Science, Institute of Astrophysics, University of Vienna, Austria Bachelor thesis, 'Polygonal Impact Craters on Mercury', supervisor: Univ.Prof. Dr. Maria G. Firneis

Professional Career

1974	Program-development at Siemens Vienna
1980	Team-leader program-development at Siemens Vienna
1989	Project Manager at Siemens Vienna: International IT-projects in Belgium, Netherlands, Sweden, Germany, Mexico branches banking and postal services
1999	IT-Management at Siemens SGP Vienna: Introducing business software SAP
2001	Head of IT-Management at Siemens SGP Vienna
2009	Retirement

Publications

1976	W. Steiner, A. Planck and G. Weihs. Crystallographphic and Magnetic Properties of R.E.2 (Fe,Ni)17 Alloys, Journal of Less-Common Metals, 45 (1976) 143 -153
2012	G.T. Weihs, J.J. Leitner and M.G. Firneis. Polygonal Impact Craters on Mercury. 43rd Lunar and Planetary Science Conference, held March 19-23, 2012 at The Woodlands, Texas. LPI Contribution No. 1659, id.1083
2012	G.T. Weihs, J.J. Leitner and M.G. Firneis. Comparison of Polygonal Impact Craters on Mercury and on other Terrestrial Planets. EGU General Assembly 2012, held 22-27 April, 2012 in Vienna, Austria., p.3729